International Journal of Nanomedicine

Dovepress

open access to scientific and medical research

Open Access Full Text Article

ORIGINAL RESEARCH

Natural Baicalein-Rich Fraction as Radiosensitizer in Combination with Bismuth Oxide Nanoparticles and Cisplatin for Clinical Radiotherapy

Noor Nabilah Talik Sisin[1], Nor Fazila Che Mat[1], Raizulnasuha Ab Rashid[1], Norhayati Dollah[2], Khairunisak Abdul Razak[3], Moshi Geso[4], Merfat Algethami[5], Wan Nordiana Rahman[1]

[1]School of Health Sciences, Universiti Sains Malaysia, Kubang Kerian, Kelantan, Malaysia; [2]Department of Nuclear Medicine, Radiotherapy and Oncology, Hospital Universiti Sains Malaysia, Kubang Kerian, Kelantan, Malaysia; [3]School of Materials and Mineral Resources Engineering, Universiti Sains Malaysia, Nibong Tebal, Penang, Malaysia; [4]School of Health and Biomedical Sciences, RMIT University, Bundoora, VIC, Australia; [5]Faculty of Science, Taif University, Al Hawiyah, Taif, Saudi Arabia

Correspondence: Wan Nordiana Rahman, School of Health Sciences, Universiti Sains Malaysia, Kubang Kerian, Kelantan, Malaysia, Tel +6097677811, Email wandiana@usm.my

Purpose: Chemotherapy has been used in conjunction with radiation therapy to improve the treatment outcomes of cancers. Cisplatin (Cis) is a standard treatment that has been used as a chemotherapeutic drug in medical settings. However, the possibility of complications constrains the treatment due to the exposure of healthy organs to unnecessary radiation and the drugs' toxicities. As a result, researchers have been looking for non-toxic chemotherapeutic agents which can be used as radiosensitizers, possibly produced from natural derivatives and nano sized materials.

Methods: BRF, Cis, and BiONPs were irradiated individually and in combinations with 6 MV of photon beam and 6 MeV of electron beams with 0 to 10 Gy radiation doses on MCF-7, MDA-MB-231, and NIH/3T3 cell lines. Then, the experimental sensitization enhancement ratios (SER) of each treatment obtained were compared to the theoretical dose enhancement factor (DEF). The interactions within the BRF-BiONPs (BB) and BRF-Cis-BiONPs (BCB) combinations were also estimated using the Combination Index (CI).

Results: BRF induced radiosensitization in all cells under 6 MV photon beam (SER of 1.06 to 1.35), and MDA-MB-231 cells only under 6 MeV electron beam (SER = 1.20). The highest SER values for BiONPs and Cis were obtained from MCF-7 cells under a 6 MeV electron beam (SER of 1.50 and 2.24, respectively). The theoretical DEFs were generally lower than the experimental SERs. Based on the SER and CI relationships, it was estimated that BB and BCB therapy methods interacted in either a synergistic or additive manner.

Conclusion: The BRF is found to induce relatively less radiosensitization effects compared to the BiONPs and Cis. The BB and BCB combinations have shown better effects with potential for becoming competently suitable radiosensitizers in breast cancer therapies.

Keywords: baicalein, bismuth oxide, nanoparticles, cisplatin, radiosensitization, synergism

Introduction

Radiotherapy (RT) is one of the cancer therapies along with surgery, chemotherapy, immunotherapy, hormone therapy, targeted therapy, stem cell transplant, and precision medicine, as specified by the International Agency for Research on Cancer (IARC) and the National Cancer Institute (NCI).[1,2] There are currently around 7600 RT centers across the world.[3] The International Atomic Energy Agency (IAEA) also stated that RT could be provided alone or in conjunction with chemotherapy and after surgery in cancer treatment programs.[3]

Breast cancer accounted for up to 2 million new cancer cases worldwide in 2018, roughly matching the number of lung cancers, followed by colorectal, prostate, and stomach cancers.[1,4] Breast cancer is the principal source of death in 103 nations for women.[4] Northern Europe, Western Europe, New Zealand, and Australia had the most significant occurrence frequency.[5] Clinically, various cancer cell subtypes would necessitate different treatment techniques, with

Received: 12 April 2022
Accepted: 19 June 2022
Published: 2 September 2022

more focused therapies preferred.[1] Chemotherapy, hormone therapy, and surgery are the most common treatments for breast cancer.[6] However, the IAEA also stated that RT might be used as the primary treatment if patients choose not to undergo surgery.[3] For breast cancer patients, the standard mode of RT is to use hypofractionated whole-breast RT for at least a month.[7] Hypofractionated RT can be delivered using brachytherapy with an interstitial or single-source balloon catheter, 3D conformal treatment with an external beam, or intraoperative treatment.[8]

Chemotherapy has been used with RT to improve the treatment performance of specific malignancies, and this combination is known as chemoradiotherapy (CRT). Gemcitabine, doxorubicin, and cisplatin are the most often used chemotherapeutic medicines as radiosensitizers.[9,10] Cisplatin (Cis) is a conventional medicine that has been utilized as a chemotherapeutic agent in clinical settings. A chemotherapeutic drug, like Cis, might potentially act as a radiosensitizer, increasing the amount of radiation administered to the tumor site. As a result, therapy might be carried out with a lower radiation dose, reducing the adverse effects on normal cells. However, the potential benefit of concurrent CRT is limited by the risk of complications owing to the exposure of high dose rate radiation to healthy organs and the toxicities of the drugs. As a result, researchers have been probing non-toxic chemotherapeutic drugs that may also be utilized as radiosensitizers during radiotherapy.

The use of plant leaves as a natural-based drug would also boost its appeal because natural-based treatments were believed to have minimal toxicity in vitro and in vivo investigations.[11–14] The medicinal phytochemicals may cause cancer cell death by inducing anticancer mechanisms such as apoptosis[15,16] and cell cycle arrest.[17,18] Because plant sources offer such promising benefits for cancer therapies, the chemicals found in plants may enhance the activities of cancer therapy,[19] particularly as a CRT drug or a radiosensitizer. For example, *Oroxylum indicum* (OI) leaves extract has been validated to induce anticancer, anti-virus, antioxidant, and radiosensitization effects.[12,13] Although OI leaves extract has radiosensitizing capabilities, it is uncertain if a recently obtained baicalein-rich fraction (BRF) from the same plant has the resembling effects due to the multiple components of compounds in the BRF.

In addition, nanoparticle-based radiosensitizers have also been introduced to expand CRT's therapeutic window as an alternative to synthetic drugs like cisplatin. The presence of radiosensitizers, such as nanoparticles (NPs), in a tumor would aid in the local absorption of radiation energy and concentrate a higher dosage at the target region, contributing to DNA damage in cancer cells.[20] A few metallic elements, such as gold, superparamagnetic iron oxide, platinum, and bismuth NPs, had shown potential to be radiosensitizers in pre-clinical studies.[20–23] Bismuth oxide (Bi_2O_3) NPs (BiONPs) have also been studied as a possible radiosensitizer.[24–26] The physical rationale is that an increase in radiation interaction may occur owing to the bismuth's high atomic number (Z = 83), which might cause more photons absorption and electron release even when low radiation energy is applied.[24,27] In addition to their appealing biocompatibility profile, the potential of BiONPs as radiosensitizers has been studied in vitro, in vivo, and in silico and phantom experiments under several clinical radiotherapy beams with promising findings.[24,26–31]

Furthermore, most earlier studies on natural compounds focused solely on the effects of individual natural compound[32,33] or a combination with NPs,[34,35] but the current study included three components as potential radiosensitizers, involving BRF, BiONPs, and Cis. Triple drug-based chemotherapy research in cancer treatment has been clinically proven to improve cancer responses compared to combining two drugs.[36,37] However, each medicine has side effects, and combining pharmaceuticals might amplify unwanted systemic effects.[38] Kareliotis et al have analyzed numerous current cancer therapy options and found that there is a need for multimodal treatment that requires the synergy of ionizing radiation and sensitizing drugs.[39]

This study looked at the combination of (1) natural BRF with BiONPs (BB) and (2) the combination of BRF, Cis, and BiONPs (BCB) to boost anticancer activities in breast cancer cells while minimizing toxicity. Previously, we had evaluated the effect of individual BRF, BiONPs, or Cis, and the combination of BiONPs with Cis (BC) on MCF-7 cells under ^{192}Ir HDR brachytherapy.[40–42] The double combination of BC with ^{192}Ir HDR brachytherapy could induce early apoptosis with alterations of glycolysis activity, amino acid structure disruption, and DNA/RNA fragmentation.[42] Correspondingly, the individual treatments (BRF, BiONPs, or Cis) and combination treatments (BB and BCB) had been determined to have high ROS amounts in relation to the radiosensitization effects under four clinical beams (HDR brachytherapy, proton, photon, and electron beams).[41,43]

This publication is the first to present the radiosensitization impact of each BRF, BiONPs, and Cis under photon and electron beam radiotherapy. Subsequently, the theoretical dose enhancement factors (DEFs) of BB and BCB combinations were compared to the experimental radiosensitization effects from our previous work,[41] and interactions among each component were predicted. This work aims to perceive if combinations of prospective radiosensitizers were more successful than a single radiosensitizer after clinical external beam RT, their comparisons with the theoretical dose enhancement, and their interactions in breast cancer and normal fibroblast cells.

Methods

Preparation of Baicalein-Rich Fraction (BRF)

The BRF was extracted and fractionated from OI plant leaves as reported by the previous literature.[13] The OI plant leaves had been verified with voucher number PIIUM 0276.[13] The IO leaves were dried, ground, and subjected to the Soxhlet extraction with methanol solvent (Merck, USA). The extracts were then fractionated using thin-layer chromatography (TLC, Merck, USA) with n-hexane: ethyl acetate (HmbG, Germany) as the mobile phase with 50:50 ratios. Bands from the leaves extract were detected, air-dried, and scraped on TLC sheets that paralleled the band of standard baicalein compound (Sigma-Aldrich, USA). The scraps were eluted with a few mL of methanol and dried at room temperature. The dried powder was given the name BRF since it contained only 75% of the baicalein component.[13] Before being employed in subsequent investigations, the BRF powder was diluted with dimethyl sulfoxide (DMSO) solvent as the primary stock and kept at −20°C. The flow of the BRF extraction and fractionation is depicted in Figure 1.

Preparation of Bismuth Oxide Nanoparticles (BiONPs)

The hydrothermal technique is employed to synthesize the BiONPs, as previously described and in the literature.[44–46] The synthesis began with the dilution and stirring of bismuth (III) nitrate pentahydrate ($Bi[NO_3]_3.5H_2O$, Sigma Aldrich, USA) and sodium sulfate (Na_2SO_4, Sigma Aldrich, USA) in distilled water. The yellow precipitates were centrifuged in a 50 mL tube with deionized water after chilling for 10 minutes at room temperature, then washed twice with ethanol. Finally, the precipitates were filtered and dried in an incubator at 80°C on filter paper. The BiONPs were rod-shaped,

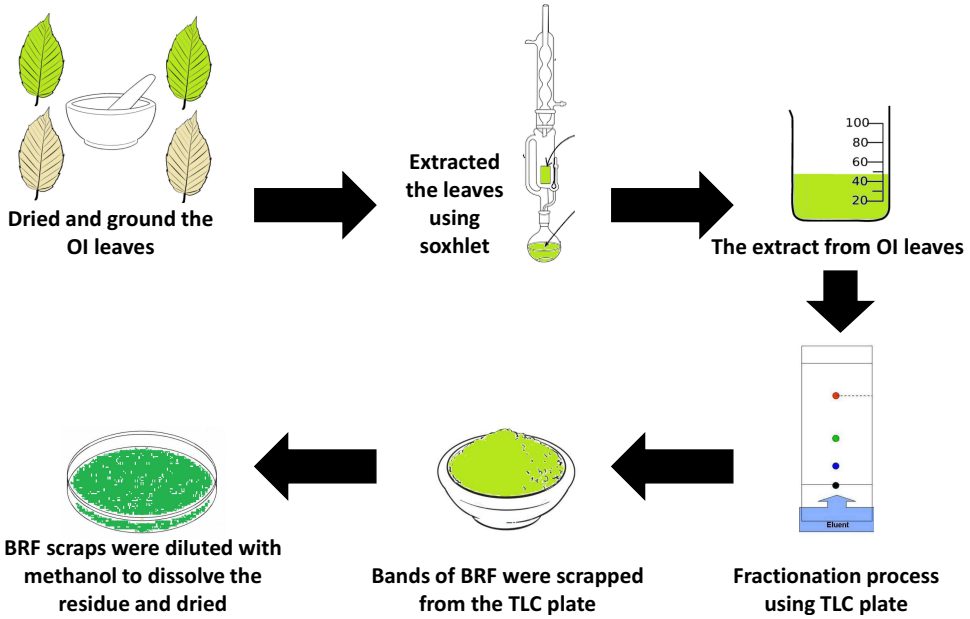

Figure 1 The processes of obtaining BRF from OI plant leaves.
Note: Data from Wahab NH, Mat NFC. Baicalein-rich fraction of oroxylum indicum leaves induces apoptosis by repressing E6 and E7 expression in HPV-associated cervical cancer cell lines. Int J Res Pharm Sci. 2018;9(SPL2):108–117.[13]

with an average diameter of 60 nm, as characterized in the prior research.[44,45] Before being employed in future investigations, the BiONPs powder was diluted with DMSO solvent as the primary stock and kept at room temperature.

Preparation of Cisplatin (Cis)

Cisplatin ($PtCl_2(NH_3)_2$, Tokyo Chemical Industry, Japan) was diluted to a concentration of 33.33 mMol/L (mM) in a 1.5 mL tube with DMSO solvent as the primary stock. This concentration was further diluted to achieve the required concentration.

Cell Culture Protocols

The MCF-7 (human breast adenocarcinoma), MDA-MB-231 (human mammary gland cancer), and NIH/3T3 (mouse embryonic fibroblast) cell lines, which were commercially purchased from ATCC®, were employed. They were grown in Dulbecco's Modified Eagles Medium (DMEM) (Gibco, USA or Nacalai Tesque, Japan) supplemented with 5% fetal bovine serum (FBS, Gibco, USA) and 1% penicillin-streptomycin (Gibco, USA). The adherent cells were detached using 0.025% trypsin-EDTA (Gibco, USA) to sub-culture the cell lines. The cells were cultured in a Galaxy cell incubator (Eppendorf), humidified with 5% carbon dioxide (CO_2), and kept at 37°C.

Cytotoxicity Assay

According to our earlier studies, the cytotoxicity tests for the BRF natural compound were conducted.[47,48] DMSO was used to dissolve the BRF. Each cell line was seeded overnight in 96-well plates and treated with two-serial dilutions of the BRF ranging from 0.39 to 100 µg/mL in wells in triplicates. The well plates were incubated at 37°C for 5 minutes with 5% CO_2. After 48 hours, the viability of each cell was determined using the Prestoblue™ test, with 10 µL of Prestoblue reagent (Invitrogen, USA) and 90 µL of fresh DMEM and incubated for 4 hours. The fluorescence was measured using a microplate reader (Varioskan Flash, ThermoFisher Scientific, US) at a wavelength of 535 nm for excitation and 615 nm for emission. The Dose-Response model graphs were fitted using OriginLab Pro 2018 (OriginLab Corporation, US). The mean ± standard error of the means (SEM) of the triple samples expresses all the data. Meanwhile, the cytotoxicity assay of BiONPs and Cis had been reported in our previous research.[40]

Cell Samples Irradiation

The samples were irradiated at the Nuclear Medicine, Radiotherapy and Oncology Department, Hospital Universiti Sains Malaysia. The irradiations of megavoltage photon and electron beam were conducted using Siemens Primus medical linear accelerator (Siemens Medical Systems, USA).

Treatment Components

Table 1 shows the results of our investigation into the impacts of six therapy components. The concentrations of each component were chosen based on our previous cytotoxicity experiments. The concentration of BRF (0.76 µg/mL) was

Table 1 Details of Treatment Components in This Study

Treatment	Components
Negative control	No treatment (cells only)
Positive control	Irradiation with 6 MV of the photon beam or 6 MeV of the electron beam (doses of 0 −10 Gy)
BRF	0.76 µg/mL of BRF
BiONPs	0.5 mM of 60 nm of BiONPs[40]
Cis	1.30 µM of Cis[40]
BB	0.76 µg/mL of BRF + 0.5 mM of BiONPs[41]
BCB	0.76 µg/mL of BRF + 1.30 µM of Cis + 0.5 mM of BiONPs[41]

chosen based on the abovementioned cytotoxicity assay. For the 60 nm size of BiONPs, a cytotoxicity experiment revealed that 0.5 mM is a safe dose, and Cis concentration was chosen based on its respective IC_{25} value of 1.30 μM, as reported in our previous research.[40] The IC_{25} was used instead of the IC_{50} to limit the side effects of each BRF and Cis and emphasize the combined effects in the future study.[49]

The treatment components were co-cultured with the cells for one hour before irradiation, with a total sample suspension volume of 150 μL in PCR tubes. Triplicate samples were taken for each of the treatment components. Gafchromic™ EBT3 films (Ashland Specialty Ingredients, USA), which were placed beneath the cell sample tubes, were used to verify radiation dosages.

Megavoltage Photon Beam Therapy

The cells were suspended in the 200 μL of PCR tubes at a 1×10^5 cells/mL concentration before getting treated upon each treatment element. Before being exposed to a 6 MV photon beam, the cell samples were put between a superflab bolus (CIVCO® Radiotherapy, USA) and a 10 cm water equivalent phantom (Nuclear Associates Inc., USA) for backscatter, with a depth of maximum dosage (d_{max}) of 1.5 cm for a field size of 10 cm x 10 cm. The radiation doses varied from 0 to 10 Gy, with a source-to-surface distance (SSD) of 100 cm.

Megavoltage Electron Beam Therapy

Cell suspensions were prepared in 200 μL PCR tubes at a density of 1×10^5 cells/mL before being treated in triplicates with each treatment component. For a 10 cm × 10 cm applicator, the tubes were arranged with an SSD of 100 cm and a d_{max} of 1.4 cm. The samples were subjected to a 6 MeV electron beam with a 10 cm water equivalent phantom for backscatter and radiation doses ranging from 0 to 10 Gy.

Post-Irradiation Clonogenic Assay

All cell suspensions were seeded onto 6-well plates without washing away the treatment components after the irradiations, with 1.5 mL of new media added to each well. MCF-7 and NIH/3T3 cells were incubated for five days, while MDA-MB-231 cells were incubated for ten days to ensure that the cell colonies developed appropriately, based on the control cells' growth efficiency. After that, the cells in the well plate were gently rinsed, fixed for 30 minutes with cold methanol, and stained for 1 hour with 1% of crystal violet. Then, the plates were rinsed again and air-dried. A flatbed scanner (Epson SeikoCorp, Japan) was used to scan the cell colonies. The picture of colony formation in the wells was processed using ImageJ software with the ColonyArea plugin developed by Guzman et al[50] to calculate the proportion of the area covered by dyed cells. The ratio of colony formation after radiation exposure to the control colonies that were not exposed to radiation was used to compute survival fractions.

Cell Survival Analysis and Radiosensitization Effects Measurement

The cell survivals were evaluated using Equation 1 to get the cell colonies' survival fraction (SF).

$$SF = \frac{\%\ of\ area\ covered\ by\ the\ irradiated\ cell\ colonies}{\%\ of\ area\ covered\ by\ the\ control\ cell\ colonies} \quad (1)$$

The SF for samples with and without therapies were then plotted and fitted using OriginLab Pro 2018 software to the LQ model,[41,51] a gold standard for fitting survival curves in clinical RT. Finally, means and SEM of triple samples are used in expressing the data.

The sensitization enhancement ratio (SER), which demonstrated amplification of radiation effects by each treatment in cells, was used to quantify the experimental radiosensitization effects from the cell survival curves. The SER was computed by dividing the dosage that causes a 50% cell survival fraction (D_{50}) for control cells by D_{50} for treated cells, as shown in Equation 2.

$$SER_{50} = \frac{D_{50,\ control}}{D_{50,\ treatment\ component}} \quad (2)$$

Theoretical Dose Enhancement Factor Calculation

The theoretical dose enhancement factors (DEF) referred to the predicted monoenergetic dose enhancement values that could be computed using several formulas.[52,53] The DEF values utilized in this investigation were calculated using the ratio of the mass-energy absorption coefficient $\left[\frac{\mu_{en}}{\rho}\right]_E$ of the BiONPs, Cis, and BRF to water, as given in Equation 3.

$$DEF = \frac{\left[\frac{\mu_{en}}{\rho}\right]_E^{water+NPs}}{\left[\frac{\mu_{en}}{\rho}\right]_E^{water}} = \frac{w_{NPs} \cdot \left[\frac{\mu_{en}}{\rho}\right]_E^{NPs} + (1 - W_{NPs}) \cdot \left[\frac{\mu_{en}}{\rho}\right]_E^{water}}{\left[\frac{\mu_{en}}{\rho}\right]_E^{water}} \quad (3)$$

where E is the energy of the monochromatic beam, and W_{NPs} is the fraction by weight of NPs in the mixture. The estimated Z_{eff} of BRF, Cis, and BiONPs were utilized as references to calculate the mass energy-absorption coefficient $\left[\frac{\mu_{en}}{\rho}\right]_E$ for each compound from the National Institute of Standards and Technology database's physical data references. The Z_{eff} of BRF, Cis, and BiONPs had been calculated in our previous research, which are 6, 62, and 78, respectively.[40,54] These Z_{eff} values are approximate to carbon, samarium, and platinum metals, respectively.

Only photon emitters such as radionuclides, LINAC photon beams, and diagnostic x-rays can be calculated theoretically. The electron, on the other hand, is a charged particle. Therefore, only the theoretical DEF for two sources, the HDR brachytherapy with an average energy of 0.38 MeV and the 6 MV photon beam with an effective photon energy of 2.0 MeV, was examined in this work concerning each treatment component.[55–58]

Combination Treatments Analysis of Synergism/Antagonism

Various approaches are utilized to analyze the interactions in the combination of several agents or stressors, including those based on the median-effect principle and its mass-action law, Bliss Independence, Loewe Additivity, directional classification system, Constant-Dose Method, and Constant-Efficacy Method.[59–62]

According to prior research on CRT, the interaction of different anticancer agent combinations could be established using the CompuSyn program (ComboSyn, Inc., Paramus, USA).[63–70] The Combination Index (CI) analysis was founded on Chou-CI Talalay's Theorem based on a computer analytical simulation of the median-effect principle and its mass-action law.[61,71] Many radiosensitization studies used this approach since it is simple, inexpensive, and primarily produces quantitative data.[63–65,67,69,72–74] The software was loaded with doses (radiation doses, Gy) and effects (SF) for each individual and combination therapy. The software then generated the data for CI values for each radiation dose. Finally, the average CI values were calculated.

Results and Discussion

Cell Viability of BRF

The cell survival curves after 48 hours of BRF treatment are shown in Figure 2. The BRF was observed to be highly toxic to MCF-7 and MDA-MB-231 breast cancer cells but demonstrate less toxicity to NIH/3T3 normal cells. The IC_{50} values for MCF-7, MDA-MB-231, and NIH/3T3 were determined using cell viability curves which resulting in values of 11.99, 26.53, and 80.53 µg/mL, respectively. Meanwhile, the IC_{25} values calculated for MCF-7, MDA-MB-231, and NIH/3T3 were 0.76, 3.99, and 32.58 µg/mL, respectively. Therefore, the lowest dose of 0.76 µg/mL from IC_{25} was used for the following tests. This value is only 0.007% differed from the lowest IC_{25} value found in our prior work.[47]

In this study, the BRF from the OI plant was evaluated as an alternative to the commercial anticancer drug as a lower cytotoxic radiosensitizer. Based on previous published research regarding the BRF, there are more works on the OI plant extracts in comparison to pure baicalein compound. Therefore, some discussions will be consociated with the OI extracts and baicalein compound. The IC_{50} value is the gold standard to speculate about the anticancer effect of plant extracts. A treatment agent with an IC_{50} value of less than 30 µg/mL could be considered an anticancer agent.[48] The BRF showed high toxicity on the breast cancer cells MCF-7 (11.99 µg/mL) and MDA-MB-231 (26.53 µg/mL) cells, while not toxic to NIH/3T3 normal cells (80.53 µg/mL). The results are supported by another study on the anticancer properties of BRF towards HeLa and SiHa cells which exhibited IC_{50} of 2.41 and 7.62 µg/mL, respectively.[13]

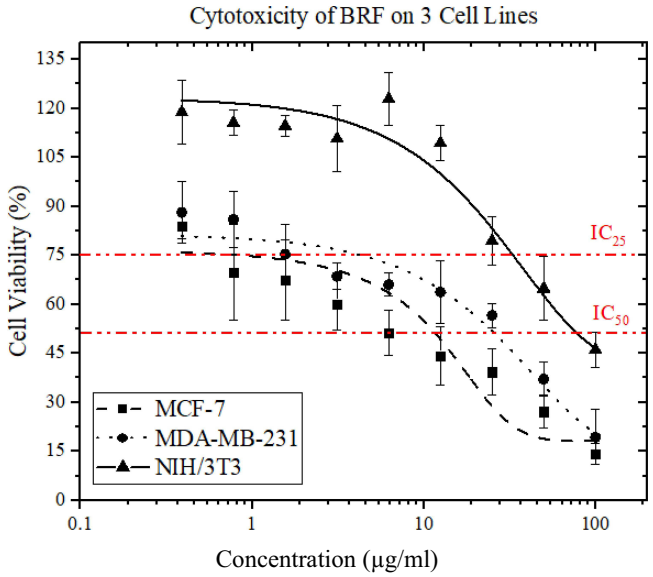

Figure 2 BRF's cytotoxicity was investigated using MCF-7, MDA-MB-231, and NIH/3T3 cell lines. Each point shows the average proportion of viable cells in contrast to the negative control. Dashed lines denote the IC_{25} and IC_{50} levels. To fit the curves, the Dose-Response model is utilized. The error bars represent the SEM.

Several pathways activated the anticancer effects of OI extracts and baicalein on cancer cells. In MCF-7 and MDA-MB-231 breast cancer cell lines, OI extracts were initially found to induce apoptosis.[75–77] BRF or baicalein compound would not disturb the NIH/3T3 cells' proliferation.[13,78] Comparable to the present study, the pathways involved might include the increment of p53 genes and the decrease of cyclinD1, vascular endothelial growth factor (VEGF), CDK4 genes, and collagen-synthesis-related proteins such as α-smooth muscle actin, collagen-1, and collagen-3 gene expressions.[78] The mechanisms might also happen in the present study, which determined the low toxicity effect of the BRF. The cytoselectivity of an agent towards different cells is an excellent characteristic of a potent anticancer agent.

Finally, this study also addressed the IC_{25} value of BRF as complementary to Cis results in the previous study, which also used the IC_{25} value.[40] Thus, the lowest concentration of 0.76 μg/mL from IC_{25} values was chosen as one of the components for the subsequent experiments. The present study only discussed the cell viability after the treatment with BRF. The cell viability after BiONPs and Cis treatments had been reported in our previous research,[40] and the results are mentioned in Table 1.

SER of Individual Components BRF, BiONPs, and Cis

Figures 3–5 show the cell survival curves after MCF-7, MDA-MB-231, and NIH/3T3 cell lines were treated with BRF, BiONPs, and Cis before exposing them to the 6 MV of a photon beam (Figure 3), 6 MeV of the electron beam (Figure 4), and HDR brachytherapy with ^{192}Ir source (Figure 5). Table 2 shows all the SER values produced when each component was treated on the three cell lines.

A combination of photon beam irradiation and BRF induced cellular sensitization with SER values of 1.06, 1.08, and 1.35 for MCF-7, MDA-MB-231, and NIH/3T3 cells, respectively. In electron beam, BRF treatment caused greater cell death in MDA-MB-231 cells than the control with an SER of 1.20, but MCF-7 cells (SER of 0.9) and NIH/3T3 cells (SER of 0.63) showed good cell survival with the survival curves above the control's curves. After the MCF-7, MDA-MB-231, and NIH/3T3 cell lines were treated with BRF and exposed to HDR brachytherapy, they did not show any cellular sensitization with SER values 0.96, 0.87, and 0.60, respectively.[47]

Incubation of BiONPs with MCF-7, MDA-MB-231, and NIH/3T3 cells followed by photon beam irradiation resulted in the SER of 1.38, 1.20, and 1.15, respectively, which indicate poor cell survival compared to the SER values obtained during electron beam therapy (1.50, 1.30, and 1.49, respectively). With HDR brachytherapy, BiONPs could sensitize the MCF-7 and MDA-MB-231 cells (SER of 1.67 and 1.03, respectively) but not NIH/3T3 normal cells (SER of 0.77 only).

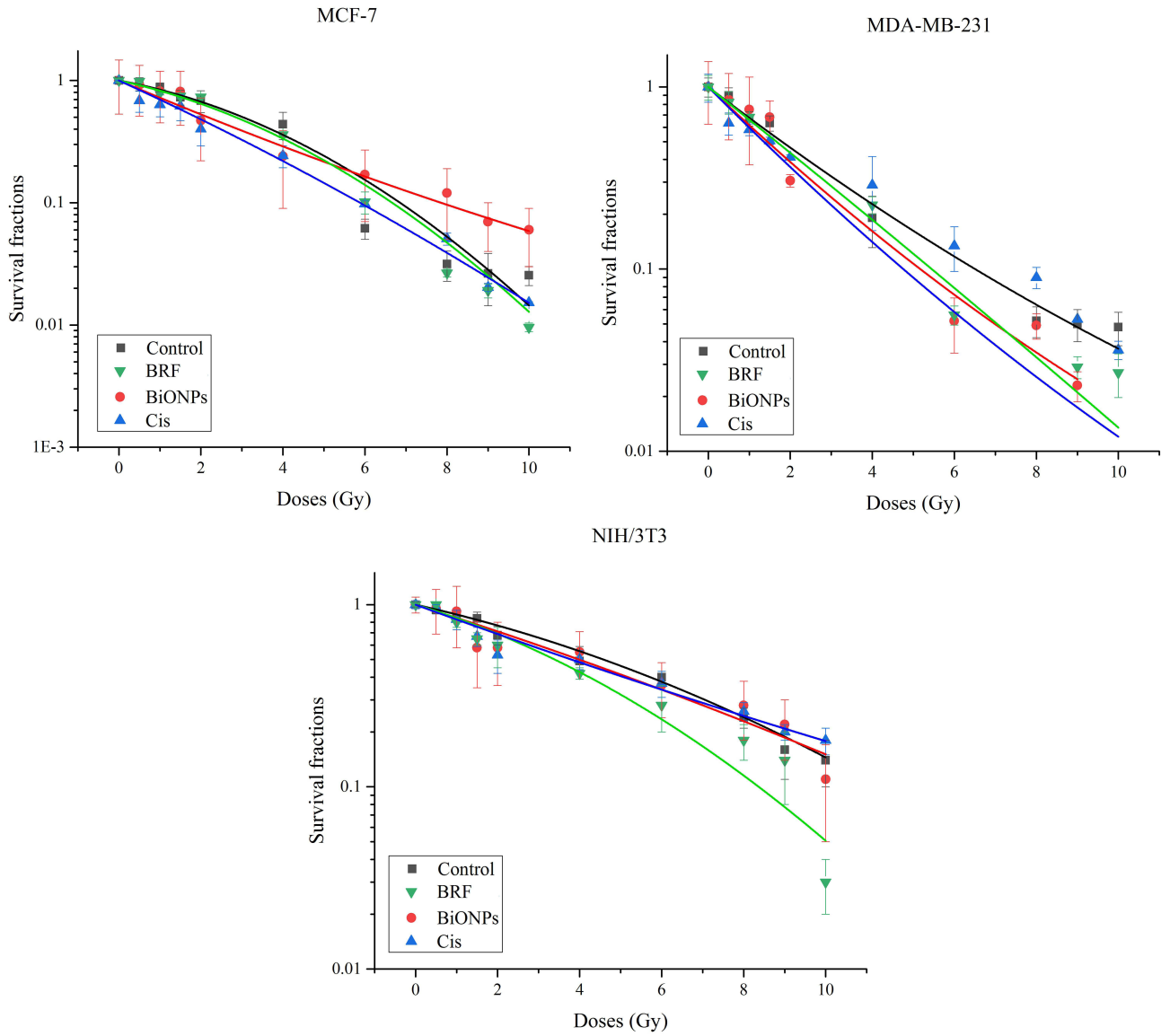

Figure 3 Survival curves of MCF-7, MDA-MB-231, and NIH/3T3 cell lines under photon beam.

In MCF-7 and MDA-MB-231 cells, Cis treatment for photon beam therapy resulted in the highest SER values of 1.60 and 1.33, respectively. The introduction of Cis during electron beam therapy exacerbated the death of MCF-7 cells with an SER of 2.24, followed by MDA-MB-231 cells with an SER of 1.80. However, in NIH/3T3 cells, the Cis did not cause radiosensitization augmentation and merely induced an SER of 0.85. The MCF-7 cells treated with Cis and HDR brachytherapy have the highest SER value of 1.70.

This study is the first to determine the effects of baicalein-based compound BRF with photon and electron beam radiations in cancer cells. However, as previously stated, the BRF in this study only contained 75% baicalein and was not a 100% pure baicalein compound, as was the case in earlier research.[79–81] As a basis, most of the discussion will focus on natural active compounds in OI plants, such as its extract, baicalein, baicalin, and oroxylin A compounds.

Overall, findings showed that when irradiated with 6 MV photon beams, BRF could sensitize all MCF-7, MDA-MB-231, and NIH/3T3 cells (SER of 1.06 to 1.35), however BRF with electron beam irradiation could only sensitize MDA-MB-231 cells (SER of 1.20). The BRF, on the other hand, was shown to offer radioprotection against HDR brachytherapy for all three cell lines (SER of 0.60 to 0.96).

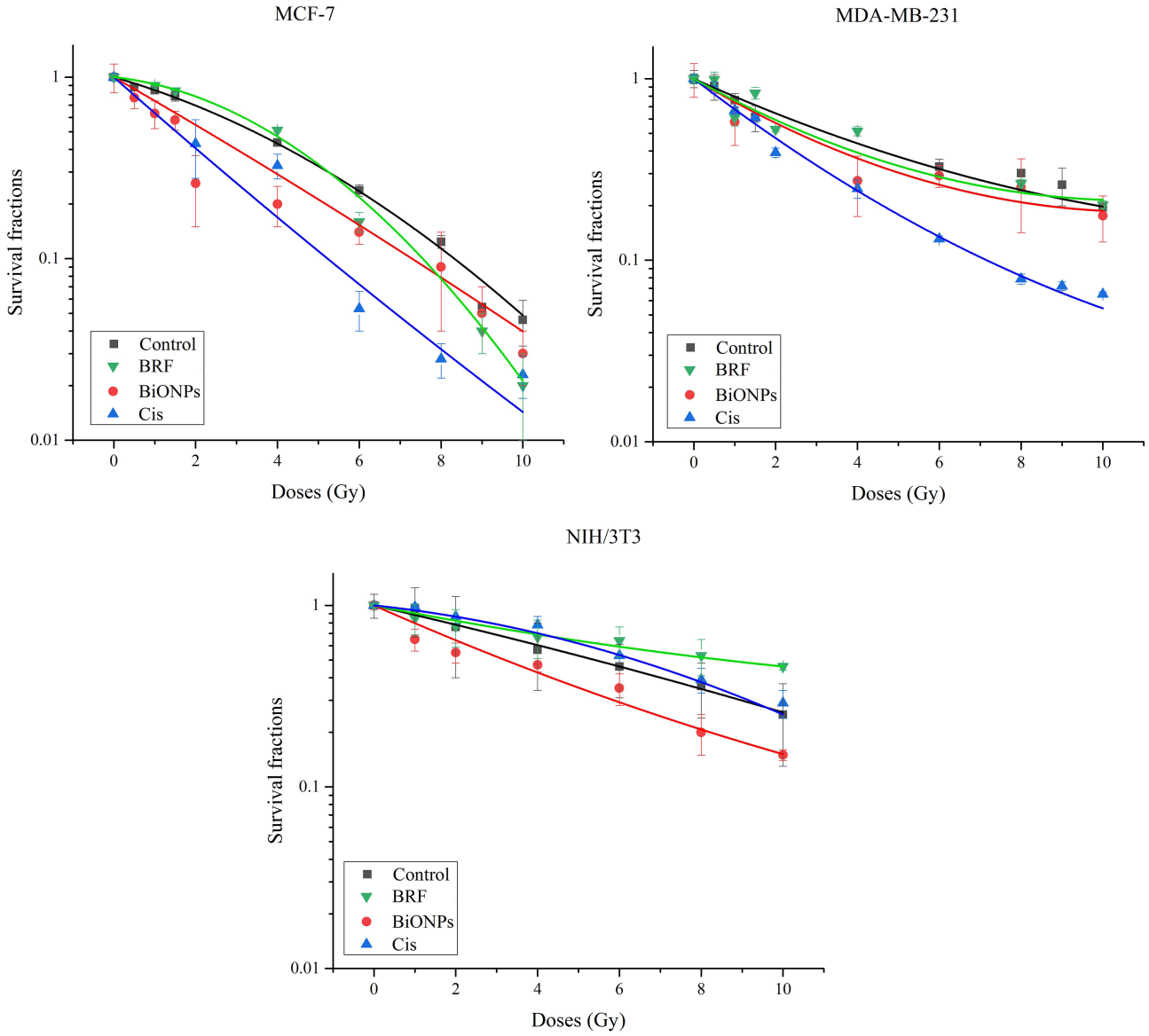

Figure 4 Survival curves of MCF-7, MDA-MB-231, and NIH/3T3 cell lines under electron beam.

Sensitization increases by BRF for 6 MV photon beam as reported in this investigation are found to be consistent with the previous studies on substances derived from OI plant extracts such as baicalin and oroxylin A.[82,83] The joined combination of baicalin compound and 6 MV photon beam irradiation sensitized CNE-2R nasopharyngeal cancer cells, whereas SER values of 1.14 to 1.25 were achieved from TE13 and ECA109 esophageal carcinoma cell lines treated with oroxylin A and X-rays.[82,83] When HeLa cervical cells with 10 µg/mL OI leaves extract were bombarded with a 6 MV photon beam, Rahman et al reported an SER of 5.00.[12] In comparison, larger extract concentrations, different cell types, or the combinatorial actions of the baicalein compound with numerous other constituents within the OI extracts might explain why the OI extracts yielded a higher SER value than the baicalin compound.[12,82,83]

Furthermore, a baicalein investigation on lung cancer cells demonstrated cellular apoptosis and autophagy via AMPK expression.[84] The stability of the Sestrins (SESN)-2 gene after irradiation stimulated AMPK signaling in MCF-7 cells, and it was initiated in dermal fibroblast cells following baicalin treatment.[85,86] However, following irradiation, AMPK expression in MDA-MB-231 cells had various effects, including inhibiting apoptosis, inducing G1 cell cycle arrest, and promoting cell growth.[87,88] The contradicting effects of AMPK pathways in different cell lines might be the causal

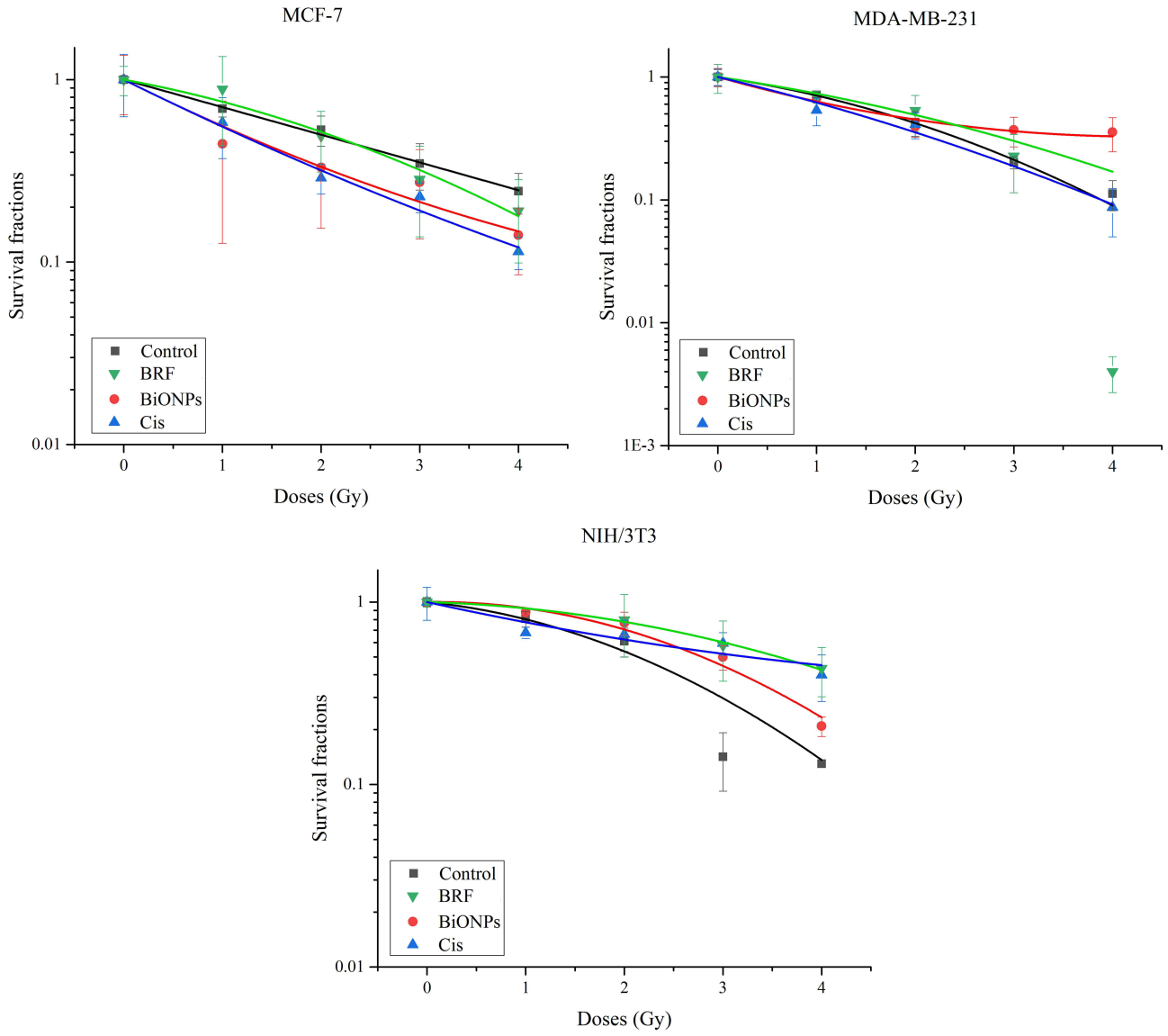

Figure 5 Survival curves of MCF-7, MDA-MB-231, and NIH/3T3 cell lines under HDR brachytherapy. The survival curves for HDR brachytherapy had been reported in our previous research[40,47] and combined in this figure for comparison.

mechanisms that occurred during electron irradiation at 6 MeV in the MCF-7, MDA-MB-231, and NIH/3T3 cells. The combination of BRF and electron beam irradiation may promote the downregulation of AMPK genes, provoking sensitization and apoptosis in MDA-MB-231 cells exclusively. However, no investigations have backed up this assertion. Further investigation utilizing immunohistochemistry, Western blotting, or PCR must be performed following the therapy to corroborate this hypothesis.

Nonetheless, natural extracts and phytochemicals have antioxidative characteristics, resulting in radioprotection. The results of an in vivo study on OI extracts irradiated with a ^{60}Co source with 1.25 MeV energy[89] were comparable and confirmed the radioprotective advantages of BRF under ^{192}Ir of HDR brachytherapy in this work. Furthermore, overexpression of AMPK genes established the radioprotective effects of baicalin compounds on skin fibroblast cells against UV A and B radiations from ROS and apoptosis.[86,90] Previous research corroborated the current findings, indicating that the BRF may perform its job as an antioxidant to overcome irradiation-induced oxidative stress, which was generated by the low energy delivered by the HDR brachytherapy. Thus, it was hypothesized that the natural agent BRF might cause radiosensitization to a lesser extent than BiONPs and Cis due to its anti-radical qualities.

Table 2 Radiobiological Analysis Based on LQ Models for Photon, Beam, Electron Beam, and HDR Brachytherapy Irradiations Corresponding to Figures 3–5

Radiations	Cell Line	Treatment	SER
6 MV (Photon)	MCF-7	BRF	1.06
		BiONPs	1.38
		Cis	1.60
	MDA-MB-231	BRF	1.08
		BiONPs	1.20
		Cis	1.33
	NIH/3T3	BRF	1.35
		BiONPs	1.15
		Cis	1.20
6 MeV (Electron)	MCF-7	BRF	0.90
		BiONPs	1.50
		Cis	2.24
	MDA-MB-231	BRF	1.20
		BiONPs	1.30
		Cis	1.80
	NIH/3T3	BRF	0.63
		BiONPs	1.49
		Cis	0.85
^{192}Ir HDR brachytherapy[40,47]	MCF-7	BRF	0.96
		BiONPs	1.67
		Cis	1.70
	MDA-MB-231	BRF	0.87
		BiONPs	1.03
		Cis	1.22
	NIH/3T3	BRF	0.60
		BiONPs	0.77
		Cis	0.66

Note: SER values for ^{192}Ir HDR brachytherapy had been reported in our previous research[40,47] and combined in this table for comparison.

The presence of BiONPs alone during RT increased the radiosensitization impact of the radiation (SER of 1.03 to 1.67), lowering cancer cell survival. The SER values for the BiONPs in the MCF-7 cells had declined following the irradiation sources; HDR brachytherapy, electron, and photon. The effect of irradiation sources on SER values for BiONPs in both MDA-MB-231 and NIH/3T3 cell lines, on the other hand, followed a similar order: electron > photon >

HDR brachytherapy. The data demonstrated that the radiosensitization effects of BiONPs were cell subtype dependent. The comparable alternating ranking of SER values seen in MDA-MB-231 and NIH/3T3 cell lines might be attributed to the qualities of MDA-MB-231 cells, which are classed as basal-like cell subtypes and reflect the characteristics of normal cells.[91] Different cell lines would suggest various tissues with varying cellular radiosensitivity.[92] Furthermore, Stewart et al had employed the identical 50 to 70 nm BiONPs on 9L cell line but under different radiation beams of 125kVp and 10 MV to induce SERs of 1.25 and 1.48, respectively.[25]

More interestingly, the SER values of BiONPs radiosensitization on MCF-7 cells in this investigation were greater than in other studies using other metal NPs under 6 MV photon beam and 6 MeV electron beam radiation energies.[93,94] Using similar MDA-MB-231 cell line, the current work on BiONPs obtained lower SER values (1.03 and 1.20 for photon and electron beams, respectively) compared to the research on gold NPs resulting in a DEF of 1.25 to 1.29 in MDA-MB-231 cells at different photon radiations.[49,95] The data might point to BiONPs being less effective than gold NPs in the triple-negative breast cancer model.

In comparison, the SER value generated by NIH/3T3 normal cells in the presence of BiONPs for HDR brachytherapy (0.77) was lower than that of photon and electron beams. These data conflicted with previous research on selenium NPs on NIH/3T3 cells which discovered a significant 85% cell survival following an 8 Gy dose of X-rays.[96] This finding validated the safe usage of individual BiONPs for HDR brachytherapy only in the future. BiONPs are a novel element in nano-research as a potential radiosensitizer, and no in vivo studies have been conducted. Nonetheless, a few studies on the radiosensitizing effects of bismuth complexes have been discovered in mice.[97–99] If the in vivo investigation was carried out, it was predicted that the BiONPs would improve the radiosensitization impact of the X-ray and electron beams on the mice.

Meanwhile, the radiosensitization effect in Cis's presence was amplified in both MCF-7 and MDA-MB-231 breast cancer cells (SER of 1.22 to 2.24) compared to NIH/3T3 normal cells (SER of 0.66 to 1.20). The maximum SERs of 2.24 and 1.70 by individual Cis treatment were seen in the MCF-7 cell line for electron beam radiation and HDR brachytherapy. The low SER values for photon beam induced by Cis in NIH/3T3 normal cell line demonstrate the low-risk effects of Cis during RT.

The interactions between Cis and electrons may cause the cleavage of the chlorine atom of the Cis molecule and the bonding of the product to the cellular DNA,[100] resulting in the high sensitization enhancement by Cis for electron beam therapy. For example, when treated with Cis and 10 KeV, a DNA double-strand breakage is reported to have an enhancement factor of 1.30.[101] Low energy electrons were used in the investigations on Cis and platinum-complex medicines.[100,101] However, energy ranging from a few MeV to a few KeV might initiate the same processes in cells.[101] Thus, the interactions may be extended to the current work, which employed high-energy ionizing radiation (6 MeV) on MCF-7 and MDA-MB-231 cells.

Moreover, the SER values of BRF, BiONPs, and Cis obtained in the present study could be compared to the intracellular ROS generations due to the presence of these individual components under ^{192}Ir HDR brachytherapy, photon and electron beams in our past research.[41] Previously, it was found that Cis could induce the highest ROS generation in each clinical beam, followed by the BiONPs and BRF,[41] similar to the SER values in this study. Therefore, these comparisons of the ROS production and the SER values could further confirm that ROS induction is one factor in the radiosensitization effects in cancer cells.

Even though Cis is a good radiosensitizer, a few experiments on kidney cells demonstrated that it causes nephrotoxicity.[102,103] As a result, the investigation, as mentioned earlier, on BRF and BiONPs as an alternative to low-toxic radiosensitizer derived from natural plant and metal NPs were also conducted in this current study. Then, the BRF, BiONPs, and Cis were mixed to form two other treatment combinations, BRF-BiONPs (BB) and BRF-Cis-BiONPs (BCB), as stated in Table 1.

The SER values of the BB and BCB had been mentioned and discussed in our previous published work.[41] It was verified that BB combinations could cause radiosensitization for the MCF-7, MDA-MB-231, and NIH/3T3 cells under all photon and electron beams, as well as brachytherapy (SER of 1.18 to 1.80) except for NIH/3T3 normal cells for the brachytherapy (SER of 0.97).[41] Meanwhile, BCB combinations could induce higher SER values of 1.31 to 2.09 in all cell

lines for the three clinical RT beams.[41] Subsequently, in the present study, the SER values of BB and BCB combinations were compared to the theoretical DEFs.

Theoretical DEF Estimations

The experimental SER values derived from cell survival curves may be compared to theoretical DEF values for monoenergetic photon beams. Figure 6A depicts the typical fluctuations in the theoretical DEF generated by all treatment components versus radiation energy ranging from 0.001 to 20 MeV. At 0.05 MeV, the BCB component produced a comparable DEF value of 8.58. As a result, the maximum DEFs for BiONPs, Cis, and BB, respectively, are 4.51 at 0.04 MeV, 5.70 at 0.06 MeV, and 4.47 at 0.04 MeV. When reaching 0.1 MeV, the DEF values rapidly decrease. The BRF, on the other hand, did not reveal any peak of the theoretical DEF value. The DEF is affected by the beam energy and the Z_{eff}, as displayed in Table 3.

Figure 6B shows a zoomed-in graph of the theoretical DEF values for HDR brachytherapy at 0.38 MeV. At 0.38 MeV energy, the DEF values were steadily falling. Figure 6C shows a zoomed-in graph of the expected DEF values for

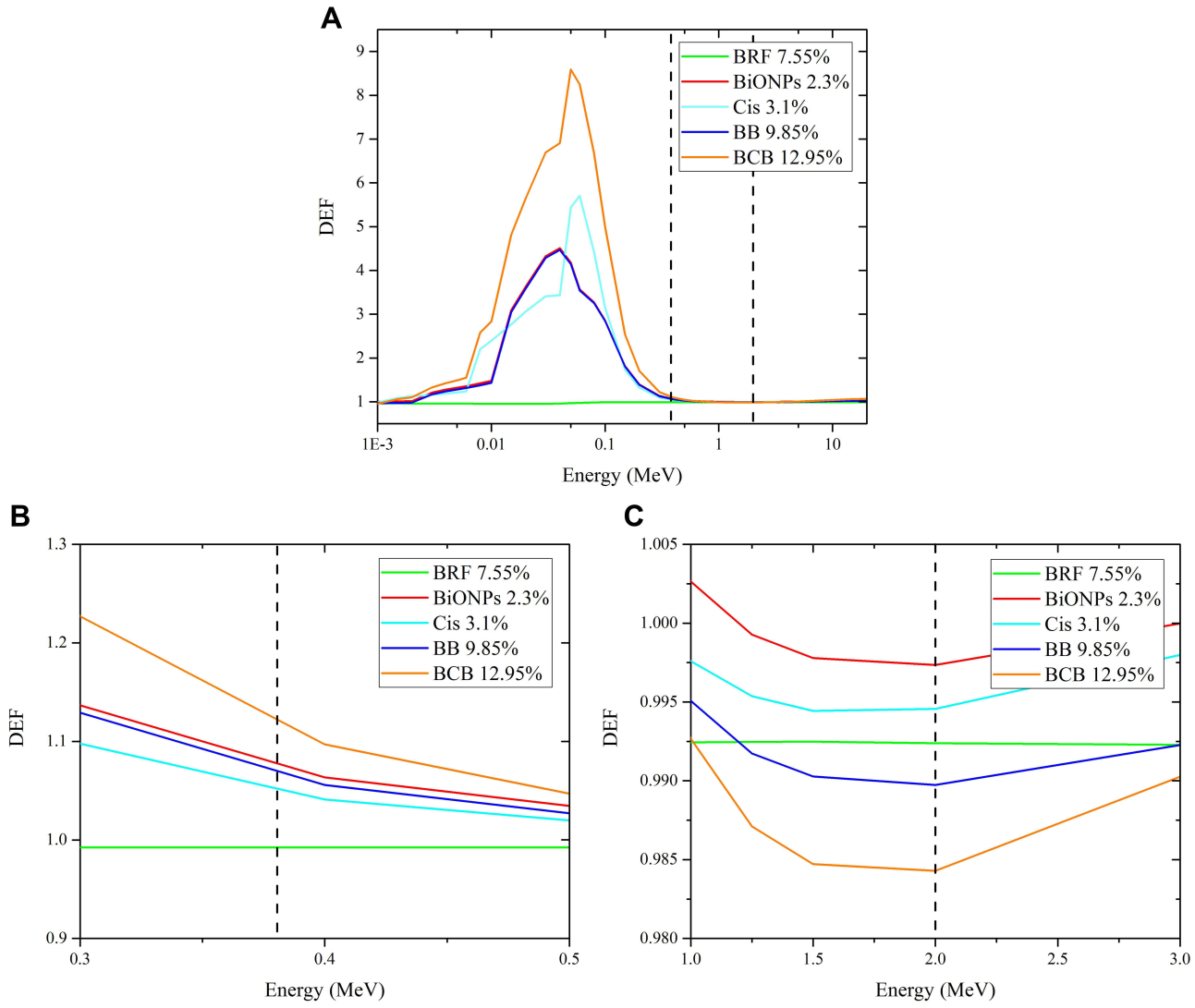

Figure 6 Theoretical DEF of each treatment component (BiONPs, Cis, BRF, BB, and BCB) (**A**) at different energy ranges from 0.001 to 20 MeV, (**B**) at 0.3 to 0.5 MeV for ^{192}Ir of HDR brachytherapy with an average energy of 0.38 MeV (the dashed line), and (**C**) at 1.0 to 3.0 for 6 MV photon beam with an effective energy of 2 MeV (the dashed line). The percentage of each component changed depending on the amount of treatment components used during irradiation.

a photon beam with an effective energy of 2 MeV at 6 MV. The lower energies' falling values ended at 2.0 MeV, and the DEF values rose moderately afterward.

Table 3 organizes the theoretical DEF values of 0.38 and 2.0 MeV obtained for each treatment component. The BCB combination was expected to provide the most substantial radiosensitization effects at 0.38 MeV, with a DEF of 1.122, followed by BiONPs alone, BB combination, and Cis alone. The BRF alone yields the smallest DEF value of 0.992 at 0.38 MeV. However, at 2.0 MeV, all the DEF values for the six treatment components were less than one.

Comparisons conducted for the estimated theoretical DEF values and the investigated experimental SER values for HDR brachytherapy are illustrated in Figure 7. Again, there is a large disparity discerned in the BCB effects. In MDA-MB-231 cells, the SER values of the BCB (1.31) treatments are higher than each theoretical DEF value (1.12) but lower than the SER values in NIH/3T3 cells (2.04).

Meanwhile, the experimental SER by BB treatment was most excellent in MCF-7 cells (1.76), followed by the SER for MDA-MB-231 cells (1.18). In general, the SER values of the BB combination were greater than the predicted DEF value (1.07), except for NIH/3T3 cells. The same pattern by cell line types may be seen in the individual Cis therapy results. The DEF of Cis treatment (1.05) fell within the experimental SER values (0.66 to 1.22).

In addition, following the individual BiONPs treatment, the experimental SER in MCF-7 cells (1.67) was larger than the theoretical DEF (1.08). The impacts of BiONPs on MDA-MB-231 and NIH/3T3 cell lines (SER of 1.08 and 0.77, respectively) were lower than their predicted DEF values.

Finally, the experimental SER values of BRF therapy in all cell lines for the brachytherapy are lower than the theoretical DEF (0.99). In the presence of BRF, the SER values of all three cell lines fell below the theoretical DEF levels.

Figure 8 depicts the differences in the DEF and SER values of the five treatment components in the three cell lines for photon beam radiation. According to the results, the experimental SER values in the MCF-7, MDA-MB-231, and NIH/3T3 cells exceeded the theoretical DEF values.

The computed DEF values for all treatment components were somewhat higher for the HDR brachytherapy, which produced less energy than the photon beam. It is consistent with previous research that found a somewhat larger dose enhancement from radionuclide sources and low-energy X-ray beams than external megavoltage-ranged beam sources.[53,93,104]

In particular, the SER values of BRF for HDR brachytherapy are lower than the DEF value, but the SER values were higher than the DEF value for photon beam therapy. The DEF values of BRF were calculated from the theoretical Z_{eff} of the BRF, which approximates a carbon element.[54] This divergence between SER values and DEF values of BRF suggested that, biologically, natural compounds could not fully mimic the actions of the carbon element. The different effects between BRF and carbon could be related to research on carbon fiber implants which found that carbon could neither increase nor decrease the radiation dose in radiotherapy.[105] Besides, the physical reaction interaction between the BRF and other components in the experiments could be less or more than the predicted reaction in the simulations.

Table 3 Theoretical DEF Values at 0.38 MeV and 2.0 MeV are Estimated from Figure 6

Treatment Component	DEF at 0.38 MeV	DEF at 2.0 MeV
BRF (0.76 μg/mL) (7.55%)	0.992[47]	0.992
BiONPs (0.5 mM) (2.3%)	1.079[40]	0.997
Cis (1.30 μM) (3.1%)	1.053[40]	0.996
BB (9.85%)	1.070	0.990
BCB (12.95%)	1.122	0.984

Notes: Some data of DEF for BRF, BiONPs, or Cis had been reported in our previous research.[40,47] The percentages were the ratio to the total volume in the cell suspensions.

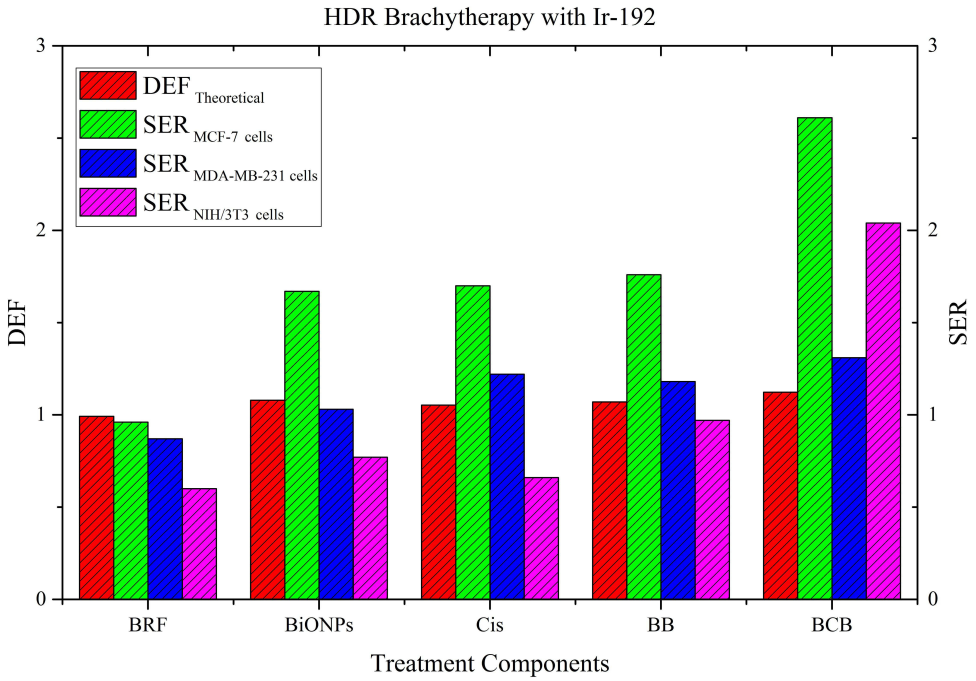

Figure 7 Comparison of theoretical DEF values and experimental SER values by each treatment component for HDR brachytherapy in MCF-7, MDA-MB-231, and NIH/3T3 cells. Theoretical DEF values are obtained from Table 3, and experimental SER values of individual BRF, BiONPs, and Cis are acquired from Table 2. The SER values of BB and BCB treatment were referred to in our prior works[41] for comparisons to the theoretical DEF.

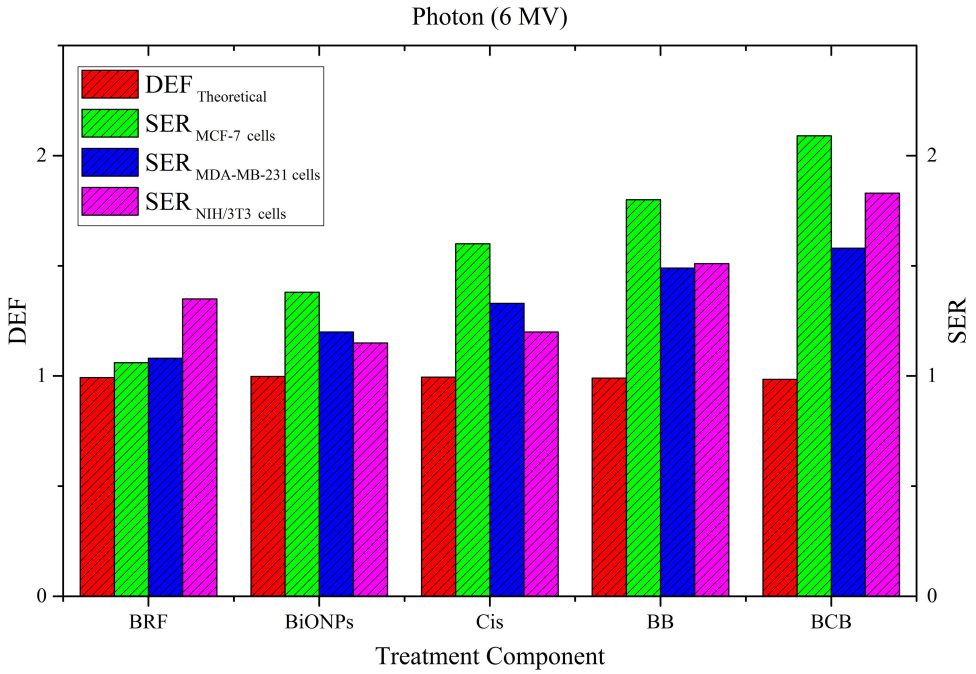

Figure 8 Theoretical DEF values and experimental SER values for photon beam therapy in MCF-7, MDA-MB-231, and NIH/3T3 cells were compared. Table 3 has the theoretical DEF values, whereas Table 2 has the experimental SER values of individual BRF, BiONPs, and Cis. In addition, SER values of BB and BCB treatment were referred to in our prior works[41] for comparisons to the theoretical DEF.

Furthermore, the experimental SERs calculated in MDA-MB-231 cells for the HDR brachytherapy in the presence of BRF and BiONPs are lower than predicted. It is supported by the fact that the MDA-MB-231 cells were shown to be radioresistant.[106,107] The radioresistance of cells was also impacted by the up- and down-regulation of proapoptotic genes such as FADD, DAPK1, CASP8, BAG-4, CASP10, NOD1, and TNFSF10.[108] However, the experimental SER of Cis,

BB, and BCB treatment components in MDA-MB-231 cells were more than 1, indicating that the radiosensitization effect was a factor in cell death. The physical interactions between BRF, BiONPs, Cis, and radiations might reduce radioresistance and promote radiosensitization to MDA-MB-231 cells.

The calculated DEF would be formed when 5 mg/mL of high-Z (20 to 90) NPs were irradiated with HDR brachytherapy, and 6 MV of photon beam was roughly 1.005 to 1.035 and 1.004 to 1.007, respectively.[53] Meanwhile, a Monte Carlo analysis on the water with 3% Cis for brachytherapy yielded a DEF of 1.07, and a Geant4 simulation with 12 mM of Cis for 6 MV energy yielded a DEF of 1.0047 to 1.0141.[109,110] The current study's theoretical DEF for the individual BiONPs and Cis differed from the studies described above. However, it could be considered consistent because the difference was less than 10%.[53] The variance in DEF might be attributed to differences in component concentration and target location depth.[24,110]

Meanwhile, when the BCB combination was present during brachytherapy, the experimental SER in NIH/3T3 normal cells was greater than the theoretical DEF, demonstrating that radiosensitization's physical, chemical, and biological routes might influence the healthy tissues surrounding the cancer sites. Nonetheless, these toxicity effects may be as minimal as the side effects of concurrent CRT in clinical research. Another brachytherapy and Cis clinical investigation discovered a few acceptable hematological and renal effects.[111] In comparison to individual brachytherapy treatment, there were greater vaginal, rectal, and bladder toxicities after a few weeks of chemobrachytherapy treatment.[112] The gap between theoretical DEF and experimental SER might be caused by a few factors, including experimental conditions and setup variables, as well as the exclusion of experimental variable circumstances in theoretical simulation.[113]

Combinatorial Treatment Analysis for BB and BCB Combinations

The effects of the combination therapies were examined using a computational analytical simulation to determine the potential interaction. The CompuSyn program was used to simulate the radiation doses and SF values of the therapy components in breast cancer cells and normal fibroblast cells to assess the synergistic, additive, and antagonistic effects of the BiONPs, Cis, or BRF for the BB and BCB combinations. Based on the CI values, the combined therapy can be regarded as synergistic (CI < 0.9), additive (CI of 0.9 to 1.2), or antagonistic (CI > 1.2). The summary of mean CI values quantified from the BB and BCB combination treatments for photon and electron beams, as well as brachytherapy, are shown in Table 4, in comparison to the SER values obtained from our previous work.[41]

BB and BCB combinations demonstrated synergistic interactions (CI < 0.9) in MCF-7 breast cancer cells and NIH/3T3 normal cells under irradiation of 6 MV photon beam with the CI average of 0.58 to 0.82. However, the average CI value of MDA-MB-231 cells reflected the overall additive effects of both the BB (CI = 0.98) and the BCB (CI = 1.02) treatments when paired with the photon beam. For each BB and BCB treatment combination, the additive interactions calculated in MDA-MB-231 cells would result in the lowest SER levels compared to other cells. The results indicated that photon irradiation with BB and BCB combination had greatly sensitized other cells, especially the MCF-7 cells, through synergistic and additive interactions, resulting in high SER values for each combination.

In the 6 MeV electron beam irradiation, the mean CI values in MCF-7 cells of BB and BCB therapies indicated additive effects (CI of 1.06 to 1.10). However, the CI values suggested synergism in MDA-MB-231 cells. Meanwhile, in NIH/3T3 normal cells, BB combination was estimated to induce synergism (CI = 0.72), in contrast to BCB combination, which might undergo a minor antagonistic interaction (CI = 1.33). From the estimation in our previous work,[41] its SER value of 2.06 contrasted with the weak antagonism effect. However, the detailed unpublished raw data expressed that only the lowest irradiation dose of 1.0 Gy elicited a strong antagonistic reaction. In comparison, higher irradiation doses (2.0 to 10 Gy) had elicited additive and synergistic reactions. As a result, larger doses of irradiation may significantly impact the SER value of BCB combination treatment on NIH/3T3 normal cells.

The current investigation discovered that all cell lines treated with BB and BCB combinations showed synergisms during HDR brachytherapy. The mean CI values of the BB and BCB treatments suggested synergism (CI of 0.59 and 0.64, respectively). In MDA-MB-231 and NIH/3T3 cells, the average CI values of BB and BCB treatment varied from 0.42 to 0.76, also indicating synergistic effects. This result conflicted with the SER of BB for HDR brachytherapy, which shows the SER of 0.97 as if there was no enhancement in the NIH/3T3 cells.[41] Nonetheless, according to another concept of modeling of interaction evaluation between two stressors,[62] the BB combination in NIH/3T3 cells for HDR brachytherapy is deemed to have an additive impact since the SER of BB (0.97) was greater than the SER of individual BiONPs (0.77) and BRF (0.60)

Table 4 The Averages of CI Values Indicate Synergism, Additive Effects, and Antagonism, and the SER Values Indicate the Radiosensitization Effects, of the BB and BCB Combinations

Radiation Types	Cells	BB Treatment		BCB Treatment	
		CI	SER[41]	CI	SER[41]
6 MV (Photon)	MCF-7	0.69	1.80	0.58	2.09
	MDA-MB-231	0.98	1.42	1.02	1.58
	NIH/3T3	0.82	1.51	0.72	1.83
6 MeV (Electron)	MCF-7	1.06	1.37	1.10	1.87
	MDA-MB-231	0.72	1.24	0.82	1.51
	NIH/3T3	0.71	1.67	1.33	2.06
^{192}Ir of HDR brachytherapy	MCF-7	0.59	1.76	0.64	2.61
	MDA-MB-231	0.56	1.18	0.69	1.31
	NIH/3T3	0.76	0.97	0.42	2.04

Note: The SER values of BB and BCB combination treatments were obtained from our previous work.[41]

from Table 2. Thus, it is hypothesized that the BB combination may have additive interaction. However, the reaction was unable to overcome the antioxidant capacity of the BRF, resulting in an SER value of 0.97.

Furthermore, the CI values of the BB combination in all cell lines from all RT sources indicated that there was no antagonistic interaction but only additive and synergistic interactions. This statement demonstrates that BRF may produce radiosensitization when combined with other components while being a natural molecule. This conclusion is corroborated by examining C-phycocyanin natural chemical and X-rays on colon cancer cells, which revealed synergistic effects and a DEF ranging from 1.05 to 1.63.[32]

Besides, due to the synergistic interaction of the BRF, BiONPs, and Cis, large SER values of BCB combinations for all RT sources were induced. Furthermore, Cis, coupled with other natural chemicals, such as *Ephedra alata* and *Sterculia quadrifida*, displayed synergism in 4T1 and T47D breast cell lines without irradiation, involving caspase-7 and caspase-3 activation, PARP inhibition, and anti-apoptotic Bcl2 protein downregulation.[114,115] The combination of nanofibers and two natural compounds of curcumin and chrysin on T47D breast cancer cells resulted in synergistic responses, including the regulation of caspase-7, caspase-3, p53, Bax, Bcl2, Cyclin D1, and human telomerase reverse transcriptase genes.[71]

Generally, the CI values of all treatment combinations for HDR brachytherapy were discovered to have synergistic interactions in all cell lines. For photon beam RT, the combination of BB and BCB had additive effects on MDA-MB-231 cells. In the case of electron beam RT, antagonistic interactions were found in NIH/3T3 normal cells for the BCB combination. In contrast, additive responses were found in MCF-7 cells for both BB and BCB combinations.

Conclusion

The BRF has shown a modest capability to produce radiosensitization effects than the BiONPs and Cis due to its antioxidative qualities. Most of the experimental SER values were higher than the theoretical DEF values, demonstrating the involvement of chemical and biological mechanisms instead of just physical interactions. The radiosensitization effects in BCB combinations were two-fold larger than in other individual BRF, Cis, or BiONPs and BB combination treatments. Radiosensitization effects on breast cancer cells indicate significant impact while small impact on normal cells were observed. Based on the SER and CI associations, it can be estimated that the BB and BCB therapeutic approaches had either synergistic or additive interactions, which indicates the possible potential as radiosensitizers for breast cancer treatments.

Acknowledgment

This work was funded by the Ministry of Higher Education Malaysia for Fundamental Research Grant Scheme with Project Code: (FRGS/1/2020/STG07/USM/02/2). In addition, we would like to convey our gratitude to the Central Research Laboratory, School of Medical Sciences, Universiti Sains Malaysia and Nuclear Medicine, Radiotherapy and Oncology Department, Hospital Universiti Sains Malaysia for the assistance during experimental works.

Disclosure

The authors report no conflicts of interest.

References

1. IARC. World cancer report 2014; 2014. Available from: https://publications.iarc.fr/Non-Series-Publications/World-Cancer-Reports/World-Cancer-Report-2014. Accessed April 10, 2022.
2. NCI. Types of cancer treatment. national institute of health; 2020. Available from: https://www.cancer.gov/about-cancer/treatment/types. Accessed August 16, 2020.
3. IAEA. Radiotherapy in cancer care: facing the global challenge; 2017. Available from: https://www.iaea.org/publications/10627/radiotherapy-in-cancer-care-facing-the-global-challenge. Accessed April 10, 2022.
4. The Global Cancer Observatory. Globocan 2018; 2019. Available from: https://gco.iarc.fr/today/data/factsheets/populations/900-world-fact-sheets.pdf. Accessed August 27, 2022.
5. Bray F, Ferlay J, Soerjomataram I, Siegel RL, Torre LA, Jemal A. Global cancer statistics 2018: GLOBOCAN estimates of incidence and mortality worldwide for 36 cancers in 185 countries. *CA Cancer J Clin*. 2018;68:394–424. doi:10.3322/caac.21492
6. Ganggayah MD, Taib NA, Har YC, Lio P, Dhillon SK. Predicting factors for survival of breast cancer patients using machine learning techniques. *BMC Med Inform Decis Mak*. 2019;19(1):1–17. doi:10.1186/s12911-019-0801-4
7. Evans S, Young M, Higgins S, Moran MS. Biological basis of radiotherapy of the breast. In: Bland KI, Copeland EM, Klimberg VS, Gradishar WJ, White J, editors. *The Breast: Comprehensive Management of Benign and Malignant Diseases*. 5th ed. Elsevier Inc; 2017:663–672.e2. doi:10.1016/B978-0-323-35955-9.00046-5
8. Whelan TJ, Kim DH, Sussman J. Clinical experience using hypofractionated radiation schedules in breast cancer. *Semin Radiat Oncol*. 2008;18(4):257–264. doi:10.1016/j.semradonc.2008.04.008
9. Hashemi FA, Akbari EH, Esmati E. Concurrent chemoradiation with weekly gemcitabine and cisplatin for locally advanced cervical cancer. *Asian Pacific J Cancer Prevent*. 2013;14:5385–5389. doi:10.7314/apjcp.2016.17.s3.287
10. Guo XL, Kang XX, Wang YQ, et al. Co-delivery of cisplatin and doxorubicin by covalently conjugating with polyamidoamine dendrimer for enhanced synergistic cancer therapy. *Acta Biomaterialia*. 2019;84:367–377. doi:10.1016/j.actbio.2018.12.007
11. Dinda B, Silsarma I, Dinda M, Rudrapaul P. Oroxylum indicum (L.) Kurz, an important Asian traditional medicine: from traditional uses to scientific data for its commercial exploitation. *J Ethnopharmacol*. 2015;161:255–278. doi:10.1016/j.jep.2014.12.027
12. Rahman WN, Mat NFC, Long NAC, Rashid RA, Dollah N, Abdullah R. Radiosensitizing effects of Oroxylum indicum extract in combination with megavoltage radiotherapy beams. In: *Materials Today: Proceedings*. Vol. 16. Elsevier Ltd; 2019:2072–2077. doi:10.1016/j.matpr.2019.06.094
13. Wahab NH, Mat NFC. Baicalein-rich fraction of oroxylum indicum leaves induces apoptosis by repressing E6 and E7 expression in HPV-associated cervical cancer cell lines. *Int J Res Pharm Sci*. 2018;9(SPL2):108–117.
14. Awang NA, Mat N, Mahmud K. Traditional knowledge and botanical description of edible bitter plants from besut, Terengganu, Malaysia. *J Agrobiotechnol*. 2020;11(1):32–47. doi:10.37231/jab.2020.11.1.180
15. Foo JB, Saiful Yazan L, Tor YS, et al. Dillenia suffruticosa dichloromethane root extract induced apoptosis towards MDA-MB-231 triple-negative breast cancer cells. *J Ethnopharmacol*. 2016;187:195–204. doi:10.1016/j.jep.2016.04.048
16. Wahab NH, Din NAM, Lim YY, Jamil NIN, Mat NFC. Proapoptotic activities of Oroxylum indicum leave extract in HeLa cells. *Asian Pac J Trop Biomed*. 2019;9(8):339–345. doi:10.4103/2221-1691.262080
17. Figueiredo CR, Matsuo AL, Massaoka MH, et al. Antitumor activity of kielmeyera coriacea leaf constituents in experimental melanoma, tested in vitro and in vivo in syngeneic mice. *Adv Pharmaceut Bulletin*. 2014;4(Suppl 1):429–436. doi:10.5681/apb.2014.063
18. Tang ELH, Rajarajeswaran J, Fung SY, Kanthimathi MS. Antioxidant activity of Coriandrum sativum and protection against DNA damage and cancer cell migration. *BMC Complement Altern Med*. 2013;13(347):1–13. doi:10.1186/1472-6882-13-347
19. Wahab NH. Elucidating the mechanism of baicalein-rich fraction from oroxylum indicum leaves in cervical cancer cell lines. PhD. Universiti Sains Malaysia; 2019. Available from: http://eprints.usm.my/48013/. Accessed April 10, 2022.
20. Rahman WN, Geso M, Yagi N, Abdul Aziz SA, Corde S, Annabell N. Optimal energy for cell radiosensitivity enhancement by gold nanoparticles using synchrotron-based monoenergetic photon beams. *Int J Nanomedicine*. 2014;9(1):2459–2467. doi:10.2147/IJN.S59471
21. Rashid RA, Abidin SZ, Anuar MAK, et al. Radiosensitization effects and ROS generation by high Z metallic nanoparticles on human colon carcinoma cell (HCT116) irradiated under 150 MeV proton beam. *OpenNano*. 2019;4(October2018):100027. doi:10.1016/j.onano.2018.100027
22. Lazim RM, Rashid RA, Pham BTT, Hawkett BS, Geso M, Rahman WN. Radiation dose enhancement effects of superparamagnetic iron oxide nanoparticles to the T24 bladder cancer cell lines irradiated with megavoltage photon beam radiotherapy. *Jurnal Sains Nuklear Malaysia*. 2018;30(2):30–38.
23. Rahman WNWA. Gold nanoparticles: novel radiobiological dose enhancement studies for radiation therapy, synchrotron based microbeam and stereotactic radiotherapy. PhD. RMIT University; 2010.
24. Taha E, Djouider F, Banoqitah E. Monte Carlo simulations for dose enhancement in cancer treatment using bismuth oxide nanoparticles implanted in brain soft tissue. *Australas Phys Eng Sci Med*. 2018;41:363–370. doi:10.1007/s13246-018-0633-z
25. Stewart C, Konstantinov K, McKinnon S, et al. First proof of bismuth oxide nanoparticles as efficient radiosensitisers on highly radioresistant cancer cells. *Physica Medica*. 2016;32(11):1444–1452. doi:10.1016/j.ejmp.2016.10.015

26. Sisin NNT, Anuar MAK, Dollah N, et al. Influence of PEG-coated bismuth oxide nanoparticles on ROS generation by electron beam radiotherapy. *Polish J Med Phy Eng*. 2022;28(2):69–76. doi:10.2478/pjmpe-2022-00xx
27. Stewart CAC. An investigation into the tailoring of bismuth oxide nanoceramic with a biomedical application as a High Z radiation enhancer for cancer therapy. Master of Science. University of Wollongong; 2014. Available from: https://ro.uow.edu.au/theses/4325/. Accessed April 10, 2022.
28. Alqathami M, Blencowe A, Geso M, Ibbott G. Quantitative 3D determination of radiosensitization by bismuth-based nanoparticles. *J Biomed Nanotechnol*. 2016;12(3):464–471. doi:10.1166/jbn.2016.2183
29. Abidin SZ, Zulkifli ZA, Razak KA, Zin H, Yunus MA, Rahman WN. PEG coated bismuth oxide nanorods induced radiosensitization on MCF-7 breast cancer cells under irradiation of megavoltage radiotherapy beams. *Materials Today Proc*. 2019;16:1640–1645. doi:10.1016/j.matpr.2019.06.029
30. Sisin NNT, Azam NA, Rashid RA, et al. Dose enhancement by bismuth oxide nanoparticles for HDR brachytherapy. *J Phys Conf Ser*. 2020;1497(012002):1–5. doi:10.1088/1742-6596/1497/1/012002
31. Sisin NNT, Abidin SZ, Muhammad Amir Y, Hafiz MZ, Razak KA, Rahman WN. Evaluation of bismuth oxide nanoparticles as radiosensitizer for megavoltage radiotherapy. *Int J Adv Sci Eng Info Technol*. 2019;9(4):1434–1443. doi:10.18517/ijaseit.9.4.7218
32. Kefayat A, Ghahremani F, Safavi A, Hajiaghababa A, Moshtaghian J. C-phycocyanin: a natural product with radiosensitizing property for enhancement of colon cancer radiation therapy efficacy through inhibition of COX-2 expression. *Sci Rep*. 2019;9(1):1–13. doi:10.1038/s41598-019-55605-w
33. Wang H, Jiang H, Corbet C, et al. Piperlongumine increases sensitivity of colorectal cancer cells to radiation: involvement of ROS production via dual inhibition of glutathione and thioredoxin systems. *Cancer Lett*. 2019;450:42–52. doi:10.1016/j.canlet.2019.02.034
34. Yu H, Yang Y, Jiang T, et al. Effective radiotherapy in tumor assisted by ganoderma lucidum polysaccharide-conjugated bismuth sulfide nanoparticles through radiosensitization and dendritic cell activation. *ACS Appl Mater Interfaces*. 2019;11(31):27536–27547. doi:10.1021/acsami.9b07804
35. Nosrati H, Charmi J, Salehiabar M, Abhari F, Danafar H. Tumor targeted albumin coated bismuth sulfide nanoparticles (Bi2S3) as radiosensitizers and carriers of curcumin for enhanced chemoradiation therapy. *ACS Biomater Sci Eng*. 2019;5(9):4416–4424. doi:10.1021/acsbiomaterials.9b00489
36. Noronha V, Patil V, Joshi A, et al. Is taxane/platinum/5 fluorouracil superior to taxane/platinum alone and does docetaxel trump paclitaxel in induction therapy for locally advanced oral cavity cancers? *Indian J Cancer*. 2015;52(1):70–73. doi:10.4103/0019-509X.175604
37. Somani N, Goyal S, Pasricha R, et al. Sequential therapy (triple drug-based induction chemotherapy followed by concurrent chemoradiotherapy) in locally advanced inoperable head and neck cancer patients - Single institute experience. *Indian J Med Paediatr Oncol*. 2011;32(2):86–91. doi:10.4103/0971-5851.89781
38. Goyal S, Pounikar T, Jain P, Arya R, Verma J. Fakhruddin. Comparison of outcome and toxicity of two different regimes of neoadjuvant chemotherapy followed by external beam radiotherapy in stages III and IV larynx and laryngopharyngeal malignancies in years 2013-2014. *J Cancer Res Ther*. 2016;12(2):920–925. doi:10.4103/0973-1482.172122
39. Kareliotis G, Tremi I, Kaitatzi M, et al. Combined radiation strategies for novel and enhanced cancer treatment. *Int J Radiat Biol*. 2020;96(9):1087–1103. doi:10.1080/09553002.2020.1787544
40. Sisin NNT, Razak KA, Abidin SZ, et al. Radiosensitization effects by bismuth oxide nanoparticles in combination with cisplatin for high dose rate brachytherapy. *Int J Nanomedicine*. 2019;14:9941–9954. doi:10.2147/IJN.S228919
41. Sisin NNT, Razak KA, Abidin SZ, et al. Synergetic influence of bismuth oxide nanoparticles, cisplatin and baicalein-rich fraction on reactive oxygen species generation and radiosensitization effects for clinical radiotherapy beams. *Int J Nanomedicine*. 2020;2020(15):7805–7823. doi:10.2147/IJN.S269214
42. Sisin NNT, Razak KA, Mat NFC, et al. The effects of bismuth oxide nanoparticles and cisplatin on MCF-7 breast cancer cells irradiated with Ir-192 high dose rate brachytherapy. *J Radiat Res Appl Sci*. 2022;15:159–171. doi:10.1016/j.jrras.2022.01.017
43. Sisin NNT, Akasaka H, Sasaki R, et al. Effects of bismuth oxide nanoparticles, cisplatin and baicalein-rich fraction on ROS generation in proton beam irradiated human colon carcinoma cells. *Polish J Med Phy Eng*. 2022;28(1):30–36. doi:10.2478/pjmpe-2022-00xx
44. Zulkifli ZA, Razak KA, Rahman WNWA, Abidin SZ. Synthesis and characterisation of bismuth oxide nanoparticles using hydrothermal method: the effect of reactant concentrations and application in radiotherapy. In: *Journal of Physics: Conference Series*. Vol. 1082. IOP Publishing; 2018:1–7. doi:10.1088/1742-6596/1082/1/012103
45. Abidin SZ. Bismuth oxide nanorods as radiosensitizers for radiotherapy. Master of Science. Universiti Sains Malaysia; 2019. Available from: http://www.mjms.usm.my/MJMS26052019/18MJMS26052019_AHS.pdf. Accessed April 10, 2022.
46. Zulkifli ZA, Razak KA, Rahman WNWA. The effect of reaction temperature on the particle size of bismuth oxide nanoparticles synthesized via hydrothermal method. 3rd International Concerence on the Science and Engineering of Materials (ICoSEM 2017) AIP Conference Proceedings 1958. Vol 020007; American Institute of Physics; 2018:1–5. doi:10.1063/1.5034538.
47. Sisin NNT, Mat NFC, Abdullah R, Rahman WN. Baicalein-rich fraction as a potential radiosensitizer or radioprotective for HDR brachytherapy: a preliminary study. *J Nuclear Related Technol*. 2020;18(1):9–16.
48. Sisin NNT, Suláin MD, Abdullah H. Antiproliferative, antioxidative and compounds identification from methanolic extract of passiflora foetida and its fractions. *J Anal Pharmaceut Res*. 2017;6(1):1–10. doi:10.15406/japlr.2017.06.00166
49. Cui L, Her S, Dunne M, et al. Significant radiation enhancement effects by gold nanoparticles in combination with cisplatin in triple negative breast cancer cells and tumor xenografts. *Radiat Res*. 2017;187(2):147–160. doi:10.1667/RR14578.1
50. Guzmán C, Bagga M, Kaur A, Westermarck J, Abankwa D. ColonyArea: an ImageJ plugin to automatically quantify colony formation in clonogenic assays. *PLoS One*. 2014;9(3):14–17. doi:10.1371/journal.pone.0092444
51. Rashid RA, Razak KA, Geso M, Abdullah R, Dollah N, Rahman WN. Radiobiological characterization of the radiosensitization effects by gold nanoparticles for megavoltage clinical radiotherapy beams. *Bionanoscience*. 2018;8(3):713–722. doi:10.1007/s12668-018-0524-5
52. Jost G, Golfier S, Pietsch H, et al. The influence of x-ray contrast agents in computed tomography on the induction of dicentrics and γ-H2AX foci in lymphocytes of human blood samples. *Phys Med Biol*. 2009;54(20):6029–6039. doi:10.1088/0031-9155/54/20/001
53. Roeske JC, Nuñez L, Hoggarth M, Labay E, Weichselbaum RR. Characterization of the theorectical radiation dose enhancement from nanoparticles. *Technol Cancer Res Treat*. 2007;6(5):395–401. doi:10.1177/153303460700600504

54. Sisin NNT, Akasaka H, Sasaki R, et al. Effects of bismuth oxide nanoparticles, cisplatin and baicalein-rich fraction on ROS generation in proton beam irradiated human colon carcinoma cells. *Polish J Med Phy Eng*. 2022;28(1):1–7. doi:10.2478/pjmpe-2022-00xx
55. Zhang M, Qin N, Jia X, Zou WJ, Khan A, Yue NJ. Investigation on using high-energy proton beam for total body irradiation (TBI). *J Appl Clin Med Phy*. 2016;17(5):90–98. doi:10.1120/jacmp.v17i5.6223
56. Kurudirek M. Water equivalence study of some phantoms based on effective photon energy, effective atomic numbers and electron densities for clinical MV X-ray and Co-60 γ-ray beams. *Nucl Instruments Methods Phy Res A*. 2013;701(2013):268–272. doi:10.1016/j.nima.2012.10.076
57. Demir F, Un A. Radiation transmission of colemanite, tincalconite and ulexite for 6 and 18MV X-rays by using linear accelerator. *Appl Radiat Isot*. 2013;72(2013):1–5. doi:10.1016/j.apradiso.2012.09.020
58. Bourland JD. Radiation oncology physics. In: *Clinical Radiation Oncology*. 4th ed. Elsevier Inc; 2015:93–147.e3. doi:10.1016/B978-0-323-24098-7.00006-X
59. Saputra EC, Huang L, Chen Y, Tucker-Kellogg L. Combination therapy and the evolution of resistance: the theoretical merits of synergism and antagonism in cancer. *Cancer Res*. 2018;78(9):2419–2431. doi:10.1158/0008-5472.CAN-17-1201
60. Tekin E, Savage VM, Yeh PJ. Measuring higher-order drug interactions: a review of recent approaches. *Current Opinion Syst Biol*. 2017;4:16–23. doi:10.1016/j.coisb.2017.05.015
61. Chou TC. Theoretical basis, experimental design, and computerized simulation of synergism and antagonism in drug combination studies. *Pharmacol Rev*. 2006;58(3):621–681. doi:10.1124/pr.58.3.10
62. Piggott JJ, Townsend CR, Matthaei CD. Reconceptualizing synergism and antagonism among multiple stressors. *Ecol Evol*. 2015;5(7):1538–1547. doi:10.1002/ece3.1465
63. Igaz N, Szőke K, Kovács D, et al. Synergistic radiosensitization by gold nanoparticles and the histone deacetylase inhibitor SAHA in 2D and 3D cancer cell cultures. *Nanomaterials*. 2020;10(1):158. doi:10.3390/nano10010158
64. Hoddinott K. In vitro evaluation of the effects of combining bisphosphonates and radiation therapy in canine osteosarcoma cells. Doctor of Veterinary Science in Clinical Studies. University of Guelph; 2017. Available from: https://atrium.lib.uoguelph.ca/xmlui/handle/10214/12159. Accessed April 10, 2022.
65. Salzwedel AO, Han J, LaRocca CJ, Shanley R, Yamamoto M, Davydova J. Combination of interferon-expressing oncolytic adenovirus with chemotherapy and radiation is highly synergistic in hamster model of pancreatic cancer. *Oncotarget*. 2018;9(26):18041–18052. doi:10.18632/oncotarget.24710
66. Cechakova L, Ondrej M, Pavlik V, et al. A potent autophagy inhibitor (Lys05) enhances the impact of ionizing radiation on human lung cancer cells H1299. *Int J Mol Sci*. 2019;20(23):5881. doi:10.3390/ijms20235881
67. Jafari S, Cheki M, Tavakoli MB, Zarrabi A, Ghazikhanlu SK, Afzalipour R. Investigation of combination effect between 6 MV X-ray radiation and polyglycerol coated superparamagnetic iron oxide nanoparticles on U87-MG cancer cells. *J Biomed Phy Eng*. 2020;10(1):15–24. doi:10.31661/jbpe.v0i0.929
68. Amoroso F, Glass K, Singh R, et al. Modulating the unfolded protein response with ONC201 to impact on radiation response in prostate cancer cells. *Sci Rep*. 2021;11(4252):1–16. doi:10.1038/s41598-021-83215-y
69. Ferreiro-Neira I, Torres NE, Liesenfeld LF, et al. XPO1 inhibition enhances radiation response in preclinical models of rectal cancer. *Clin Cancer Res*. 2016;22(7):1663–1673. doi:10.1158/1078-0432.CCR-15-0978
70. Lei G, Zhang Y, Koppula P, et al. The role of ferroptosis in ionizing radiation-induced cell death and tumor suppression. *Cell Res*. 2020;30(2):146–162. doi:10.1038/s41422-019-0263-3
71. Rasouli S, Montazeri M, Mashayekhi S, et al. Synergistic anticancer effects of electrospun nanofiber-mediated codelivery of Curcumin and Chrysin: possible application in prevention of breast cancer local recurrence. *J Drug Deliv Sci Technol*. 2020;55(101402):1–8. doi:10.1016/j.jddst.2019.101402
72. Spiegelberg D, Abramenkovs A, Mortensen ACL, Lundsten S, Nestor M, Stenerlöw B. The HSP90 inhibitor Onalespib exerts synergistic anti-cancer effects when combined with radiotherapy: an in vitro and in vivo approach. *Sci Rep*. 2020;10(1):1–11. doi:10.1038/s41598-020-62293-4
73. DuRoss AN, Neufeld MJ, Landry MR, et al. Micellar formulation of talazoparib and buparlisib for enhanced DNA damage in breast cancer chemoradiotherapy. *ACS Appl Mater Interfaces*. 2019;11(13):12342–12356. doi:10.1021/acsami.9b02408
74. Fu J, Zhang N, Chou JH, et al. Drug combination in vivo using combination index method: taxotere and T607 against colon carcinoma HCT-116 xenograft tumor in nude mice. *Synergy*. 2016;3:15–30. doi:10.1016/j.synres.2016.06.001
75. Kumar DRN, George VC, Suresh PK, Kumar RA. Cytotoxicity, apoptosis induction and anti-metastatic potential of Oroxylum indicum in human breast cancer cells. *Asian Pacific J Cancer Prevent*. 2012;13(6):2729–2734. doi:10.7314/APJCP.2012.13.6.2729
76. Buranrat B, Konsue A, Wongsuwan P. Extracts of edible, medicinal Thai plants inhibit the human breast cancer cells. *Trop J Pharmaceut Res*. 2020;19(3):595–601. doi:10.4314/tjpr.v19i3.20
77. Buranrat B, Noiwetch S, Suksar T, Ta-ut A. Inhibition of cell proliferation and migration by Oroxylum indicum extracts on breast cancer cells via Rac1 modulation. *J Pharma Anal*. 2020;1–7. doi:10.1016/j.jpha.2020.02.003
78. Yang L, Li X, Zhang S, Song J, Zhu T. Baicalein inhibits proliferation and collagen synthesis of mice fibroblast cell line NIH/3T3 by regulation of miR-9/insulin-like growth factor-1 axis. *Artif Cells, Nanomed Biotechnol*. 2019;47(1):3202–3211. doi:10.1080/21691401.2019.1645150
79. Koh SY, Moon JY, Unno T, Cho SK. Baicalein suppresses stem cell-like characteristics in radio-and chemoresistant MDA-MB-231 human breast cancer cells through up-regulation of IFIT2. *Nutrients*. 2019;11(3). doi:10.3390/nu11030624
80. Xi Q, Qi H, Li Y, Xi Y, Zhang L. Low frequency ultrasound combined with baicalein can reduced the invasive capacity of breast cancer cells by down regulating the expression of MMP-2, MMP-9, and u-PA. *Transl Cancer Res*. 2016;5(6):838–844. doi:10.21037/tcr.2016.12.11
81. Oh SB, Park HR, Jang YJ, Choi SY, Son TG, Lee J. Baicalein attenuates impaired hippocampal neurogenesis and the neurocognitive deficits induced by γ-ray radiation. *Br J Pharmacol*. 2013;168(2):421–431. doi:10.1111/j.1476-5381.2012.02142.x
82. Wang C, Yang Y, Sun L, et al. Baicalin reverses radioresistance in nasopharyngeal carcinoma by downregulating autophagy. *Cancer Cell Int*. 2020;20(1):1–8. doi:10.1186/s12935-020-1107-4
83. Tan C, Qian X, Ge Y, et al. Oroxylin a could be a promising radiosensitizer for esophageal squamous cell carcinoma by inducing G2/M arrest and activating apoptosis. *Pathol Oncol Res*. 2017;23(2):323–328. doi:10.1007/s12253-016-0106-1

84. Deng X, Liu J, Liu L, Sun X, Huang J, Dong J. Drp1-mediated mitochondrial fission contributes to baicalein-induced apoptosis and autophagy in lung cancer via activation of AMPK signaling pathway. *Int J Biol Sci*. 2020;16(8):1403–1416. doi:10.7150/ijbs.41768
85. Sanli T, Linher-Melville K, Tsakiridis T, Singh G. Sestrin2 modulates AMPK subunit expression and its response to ionizing radiation in breast cancer cells. *PLoS One*. 2012;7(2):e32035. doi:10.1371/journal.pone.0032035
86. Zhang JA, Luan C, Huang D, Ju M, Chen K, Gu H. Induction of autophagy by baicalin through the AMPK-mTOR pathway protects human skin fibroblasts from ultraviolet B radiation-induced apoptosis. *Drug Des Devel Ther*. 2020;14:417–428. doi:10.2147/DDDT.S228047
87. Liu P, Ye F, Xie X, et al. mir-101-3p is a key regulator of tumor metabolism in triple negative breast cancer targeting AMPK. *Oncotarget*. 2016;7(23):35188–35198. doi:10.18632/oncotarget.9072
88. Johnson J, Chow Z, Napier D, et al. Targeting PI3K and AMPKα signaling alone or in combination to enhance radiosensitivity of triple negative breast cancer. *Cells*. 2020;9(5):1–16. doi:10.3390/cells9051253
89. Thokchom DS, Shantikumar L, Sharma GJ. Protection of radiation-induced DNA damage in Albino rats by Oroxylum indicum (L.) Vent. *Int J Pharmacognosy Phytochem Res*. 2014;6(3):514–523.
90. Zhou BR, Yin H, Xu Y, et al. Baicalin protects human skin fibroblasts from ultraviolet A radiation-induced oxidative damage and apoptosis. *Free Radic Res*. 2012;46(12):1458–1471. doi:10.3109/10715762.2012.726355
91. Carraher CE, Michael J, Ryan RR. Synthesis and preliminary cancer cell line results for the product of organotin dihalides and Alpha-Cyano-4-hydroxycinnamic acid. *J Inorg Organomet Polym Mater*. 2016;1–11. doi:10.1007/s10904-016-0363-1
92. Patel SG, Sayers EJ, He L, et al. Cell-penetrating peptide sequence and modification dependent uptake and subcellular distribution of green florescent protein in different cell lines. *Sci Rep*. 2019;9(1):1–9. doi:10.1038/s41598-019-42456-8
93. Shahhoseini E, Ramachandran P, Patterson WR, Geso M. Determination of dose enhancement caused by AuNPs with Xoft® Axxent ® Electronic (eBxTM) and conventional brachytherapy: in vitro study. *Int J Nanomed*. 2018;13:5733–5741. doi:10.2147/IJN.S174624
94. Rahman WNWA, Rashid RA, Muhammad M, Dollah N, Razak KA, Geso M. Dose enhancement by different size of gold nanoparticles under irradiation of megavoltage photon beam. *Jurnal Sains Nuklear Malaysia*. 2018;30(2):23–29.
95. Jain S, Ch B, Coulter JA, Ph D, Hounsell AR, Karl T. Cell-specific radiosensitization by gold nanoparticles at megavoltage radiation energies. *Int J Radiat Oncol - Biol - Phy*. 2011;79(2):531–539. doi:10.1016/j.ijrobp.2010.08.044.CELL-SPECIFIC
96. Yu B, Liu T, Du Y, Luo Z, Zheng W, Chen T. X-ray-responsive selenium nanoparticles for enhanced cancer chemo-radiotherapy. *Colloids Surf B Biointerfaces*. 2016;139:180–189. doi:10.1016/j.colsurfb.2015.11.063
97. Abhari F, Charmi J, Rezaeejam H, et al. Folic acid modified bismuth sulfide and gold heterodimers for enhancing radiosensitization of mice tumors to X-ray radiation. *ACS Sustain Chem Eng*. 2020;8(13):5260–5269. doi:10.1021/acssuschemeng.0c00182
98. Zhang XD, Jing Y, Song S, et al. Catalytic topological insulator Bi2Se3 nanoparticles for in vivo protection against ionizing radiation. *Nanomed: Nanotechnol, Biol Med*. 2017;13(5):1597–1605. doi:10.1016/j.nano.2017.02.018
99. Deng J, Xu S, Hu W, Xun X, Zheng L, Su M. Tumor targeted, stealthy and degradable bismuth nanoparticles for enhanced X-ray radiation therapy of breast cancer. *Biomaterials*. 2018;154:24–33. doi:10.1016/j.biomaterials.2017.10.048
100. Kopyra J, Koenig-Lehmann C, Bald I, Illenberger E. A single slow electron triggers the loss of both chlorine atoms from the anticancer drug cisplatin: implications for chemoradiation therapy. *Angewandte Chemie - Int Ed*. 2009;48:7904–7907. doi:10.1002/anie.200903874
101. Rezaee M, Hunting DJ, Sanche L. New insights into the mechanism underlying the synergistic action of ionizing radiation with platinum chemotherapeutic drugs: the role of low-energy electrons. *Int J Radiat Oncol Biol Phys*. 2013;87(4):847–853. doi:10.1016/j.ijrobp.2013.06.2037
102. Chan S, Wang R, Man K, et al. A novel synthetic compound, bismuth zinc citrate, could potentially reduce cisplatin-induced toxicity without compromising the anticancer effect through enhanced expression of antioxidant protein. *Transl Oncol*. 2019;12(5):788–799. doi:10.1016/j.tranon.2019.02.003
103. Guo Y, Wei L, Zhou Y, et al. Flavonoid GL-V9 induces apoptosis and inhibits glycolysis of breast cancer via disrupting GSK-3β-modulated mitochondrial binding of HKII. *Free Radic Biol Med*. 2020;146(July2019):119–129. doi:10.1016/j.freeradbiomed.2019.10.413
104. Rahman WN, Bishara N, Ackerly T, et al. Enhancement of radiation effects by gold nanoparticles for superficial radiation therapy. *Nanomed: Nanotechnol, Biol Med*. 2009;5:136–142. doi:10.1016/j.nano.2009.01.014
105. Xin-ye N, Xiao-bin T, Chang-ran G, Da C. The prospect of carbon fiber implants in radiotherapy. *J Appl Clin Med Phy*. 2012;13(4):152–159. doi:10.1120/jacmp.v13i4.3821
106. Dinkelborg PH, Wang M, Gheorghiu L, et al. A common Chk1-dependent phenotype of DNA double-strand break suppression in two distinct radioresistant cancer types. *Breast Cancer Res Treat*. 2019;174(3):605–613. doi:10.1007/s10549-018-05079-7
107. Gray M, Turnbull AK, Ward C, et al. Development and characterisation of acquired radioresistant breast cancer cell lines. *Radiat Oncol*. 2019;14(1):1–19. doi:10.1186/s13014-019-1268-2
108. Gupta S, Koru-Sengul T, Arnold SM, Devi GR, Mohiuddin M, Ahmed MM. Low-dose fractionated radiation potentiates the effects of cisplatin independent of the hyper-radiation sensitivity in human lung cancer cells. *Mol Cancer Ther*. 2011;10(2):292–302. doi:10.1158/1535-7163.mct-10-0630
109. Yoon M, Cho S, Jeong JH, Kim CH. Monte carlo simulation study on dose enhancement by gold nanoparticles in brachytherapy. *J Korean Phy Society*. 2010;56(6):1754–1758. doi:10.3938/jkps.56.1754
110. Baulin AA, Sukhikh LG, Sukhikh ES. Simulation dose enhancement in radiotherapy caused by cisplatin. In: *Journal of Instrumentation*. Vol. 15. IOP Publishing for Sissa Medialab; 2020:1–16.
111. Aghili M, Andalib B, Hashemi FA, et al. Concurrent Chemo-brachytherapy with Cisplatin and intracavitary brachytherapy in locally advanced uterine cervical cancer. *CANCER Bull Cancer Inst Iran*. 2010;2:45–52.
112. Mukherjee A, Patra NB, Manir KS, Shyamal KS. A prospective clinical study on the benefit of adding chemotherapy to brachytherapy in patients with incomplete response to external beam irradiation with concurrent chemotherapy in locally advanced cases of carcinoma cervix. *Indian J Med Res Pharma Sci*. 2016;3(7):9–19. doi:10.5281/zenodo.1019549
113. Corde S, Joubert A, Adam JF, et al. Synchrotron radiation-based experimental determination of the optimal energy for cell radiotoxicity enhancement following photoelectric effect on stable iodinated compounds. *Br J Cancer*. 2004;91(3):544–551. doi:10.1038/sj.bjc.6601951
114. Sioud F, Amor S, Toumia IB. A new highlight of ephedra alata decne properties as potential adjuvant in combination with cisplatin to induce cell death of 4t1 breast cancer cells in vitro and in vivo. *Cells*. 2020;9(362):1–19. doi:10.3390/cells9020362
115. Rollando R, Prilianti KR. Sterculia Quadrifida R.Br ethyl acetate fraction increases cisplatin cytotoxicity on T47D breast cancer cells. *Int J Pharma Res*. 2018;10(3):204–212. doi:10.31838/ijpr/2018.10.03.072